DUDLEY KNOX LIBRARY
NAVAL POSTGRADUATE SCHOOL
MONTEREY CA 93943-5101

Approved for public release; distribution is unlimited.

MODELING THE SEARCH FOR A RANDOMLY MOVING TARGET BY A PATROLLING SEARCHER

by

William John Lohr
Lieutenant , United States Navy
B.S.E, University of Pennsylvania, 1985

Submitted in partial fulfillment of the
requirements for the degree of

MASTER OF SCIENCE IN OPERATIONS RESEARCH

from the

NAVAL POSTGRADUATE SCHOOL
September 1992

REPORT DOCUMENTATION PAGE

REPORT SECURITY CLASSIFICATION Unclassified	1b. RESTRICTIVE MARKINGS Unclassified
SECURITY CLASSIFICATION AUTHORITY	3. DISTRIBUTION/ AVAILABILITY OF REPORT Approved for public release; distribution is unlimited.
DECLASSIFICATION/DOWNGRADING SCHEDULE	
PERFORMING ORGANIZATION REPORT NUMBER(S)	5. MONITORING ORGANIZATION REPORT NUMBER(S)
NAME OF PERFORMING ANIZATION Naval Postgraduate School 6b. OFFICE SYMBOL *(If Applicable)* OR	7a. NAME OF MONITORING ORGANIZATION Naval Postgraduate School
ADDRESS *(city, state, and ZIP code)* Monterey, CA 93943-5000	7b. ADDRESS *(city, state, and ZIP code)* Monterey, CA 93943-5000
NAME OF FUNDING/SPONSORING ORGANIZATION 8b. OFFICE SYMBOL *(If Applicable)*	9. PROCUREMENT INSTRUMENT IDENTIFICATION NUMBER
ADDRESS *(city, state, and ZIP code)*	10. SOURCE OF FUNDING NUMBERS PROGRAM ELEMENT NO. / PROJECT NO. / TASK NO. / WORK UNIT ACCESSION NO.

TITLE *(Include Security Classification)*
MODELING THE SEARCH FOR A RANDOMLY MOVING TARGET BY A PATROLLING SEARCHER(U)

PERSONAL AUTHOR(S)
Lohr, William J.

TYPE OF REPORT	13b. TIME COVERED FROM TO	14. DATE OF REPORT *(year, month,day)*	15. PAGE COUNT
Master's Thesis		1992 September	55

SUPPLEMENTARY NOTATION
The views expressed in this thesis are those of the author and do not reflect the official policy or position of the Department of Defense or the U.S. Government.

COSATI CODES			18. SUBJECT TERMS *(continue on reverse if necessary and identify by block number)*
IELD	GROUP	SUBGROUP	Search Theory, Exhaustive Search, Random Search

ABSTRACT *(Continue on reverse if necessary and identify by block number)*
This thesis develops a model, called Area Motion Search (AMS), that determines the ection probability for a patrolling sensor searching for a randomly moving target in a fixed a. The AMS model reduces to exhaustive search when the target is stationary and to random rch when the searcher is stationary. Thus, AMS is a bridge between these two often used dels in search theory, and provides a unified treatment of both.

DISTRIBUTION/AVAILABILITY OF ABSTRACT UNCLASSIFIED/UNLIMITED ☐ SAME AS ☐ DTIC USERS	21. ABSTRACT SECURITY CLASSIFICATION Unclassified
NAME OF RESPONSIBLE INDIVIDUAL J. N. Eagle	22b. TELEPHONE (Include Area Code) (408) 646-2654 22c. OFFICE SYMBOL Code OR/Ea

ORM 1473, 84 MAR 83 APR edition may be used until exhausted SECURITY CLASSIFICATION OF THIS PAGE
All other editions are obsolete Unclassified

ABSTRACT

This thesis develops a model, called Area Motion Search (AMS), that determines the detection probability for a patrolling sensor searching for a randomly moving target in a fixed area. The AMS model reduces to exhaustive search when the target is stationary and to random search when the searcher is stationary. Thus, AMS is a bridge between these two often used models in search theory, and provides a unified treatment of both.

Library
Code 55
NPS
Monterey, CA 93943

I. INTRODUCTION 1
A. GOAL 1
B. METHODOLOGY 1
II. MODEL DEVELOPMENT 3
A. ASSUMPTIONS 3
B. DETECTION RATE DEVELOPMENT 4
C. AREA MOTION SEARCH DETECTION RATE FUNCTION 6
1. Cookie-Cutter Sensor Target Free Area 7
2. Line-sensor Target Free Area 10
3. AMS Search Rate and Dynamic Enhancement 11
4. AMS Line-sensor Detection Rate and Expected Detection Time 13
D. EMBELLISHMENTS 14
III. SIMULATION DEVELOPMENT AND VALIDATION 17
A. DESIGN CONSIDERATIONS 17
1. The Random Target 17
2. The Patrolling Searcher and the Search Area 22
B. SIMULATION VALIDATION 22
IV. DATA ANALYSIS 25
A. EXPLORATORY DATA ANALYSIS 26
B. ADVANCED DATA ANALYSIS 27
1. ETFA versus TFA 28
2. The Most Accurate Line-Sensor AMS Model 28
3. Effective Searcher Speed 31
4. ETFA versus TFA for Small $\frac{LU}{RV}$ Scenarios 35
5. Line-sensor versus Cookie-Cutter Sensor 42
V. CONCLUSIONS AND RECOMMENDATIONS 43
A. CONCLUSIONS 43

DUDLEY KNOX LIBRARY
NAVAL POSTGRADUATE SCHOOL
MONTEREY CA 93943-5101

B. RECOMMENDATIONS FOR FURTHER RESEARCH 45

REFERENCES 46

BIBLIOGRAPHY 47

INITIAL DISTRIBUTION LIST 48

I. INTRODUCTION

A. GOAL

The two most widely used models for area search are Exhaustive Search (ES) and Random Search (RS).

If searcher speed is V, detection range is R, and area size is A, then ES predicts that the time of initial detection, T, is uniformly distributed between 0 and A/2RV. This model is appropriate when the searcher attempts to cover A in an efficient, systematic fashion and the target is stationary and uniformly distributed over A.

Though RS is traditionally derived with a stationary target and a random searcher, it also covers the scenario of a stationary searcher and a random target. Therefore, if the searcher is stationary and the target is moving over A in a random fashion with speed U, then RS predicts that T will have an exponential distribution with mean A/2RU.

The goal of this thesis is to produce and test a new analytical model which is a hybrid of ES and RS. Both the searcher and target will be allowed to move. The searcher's motion will be systematic (as in ES) , and the target's motion will be random (as in RS). Both ES and RS will be special cases of the new model, called Area Motion Search (AMS).

B. METHODOLOGY

Following the development in Washburn's *Search and Detection,* [Ref. 1:pp. 2-1 - 2-4] and Koopman's *Search and Screening* [Ref. 2] a Poisson

process model will be proposed for the detection process. That is, an instantaneous detection rate $\gamma(t)$ will be introduced. Then the cumulative distribution function (cdf) of T will be

$$F(t) = 1 - \exp\left(-\int_0^t \gamma(u)du\right).$$

The analytical contribution of the thesis is the development of this detection rate model. The model will be tested against a discrete-event simulation.

Detection rate mathematics and the development of the AMS detection rate models are explained in Chapter II, Model Development.

Chapter III, Simulation Development, details the modification of LT Richard L. Darden's simulation, *Hounds and Hares*. After validation, this simulation was used to examine the AMS model. Simulation results were compared with AMS using several detection rate functions in an effort to find the best model. This process is described in Chapter IV, Data Analysis. Finally, Chapter V, Conclusions and Recommendations, summarizes and critiques the results of the data analysis chapter and presents areas that could use further research.

II. MODEL DEVELOPMENT

This chapter develops the AMS model. The Assumptions section examines the assumptions necessary to determine the detection rate function for AMS. They agree with both the ES and RS model assumptions. The Detection Rate Background section explains detection rate theory and the Area Motion Search Detection Rate Function section applies detection rate theory to the AMS scenario to determine a basic AMS model. Various model variations are discussed in the Embellishments section.

A. ASSUMPTIONS

The AMS stochastic model is based on assumptions that are consistent with the assumptions used in the ES and RS models [Ref. 1:pp. 1-2, 2-2 and Ref. 2]:

- The target is in random motion on search area A, with speed U. (In ES the target's speed U equals zero.)
- The searcher performs a systematic, non-overlapping, exhaustive search at constant speed V, over area A.
- The searcher detects the target with probability 1.0 when distance from the searcher to the target is within detection range R, and does not detect the target otherwise. (The simplest versions of classical ES and RS are actually based on a line sensor with width 2R.)
- Detection events during non-overlapping time periods are probabilistically independent.

The last assumption is the least intuitive and the most questionable. The degree to which simulation results match the model predictions will be a measure of the suitability of this assumption.

B. DETECTION RATE DEVELOPMENT

A detection rate, $\gamma(t)$, multiplied by a very small time period, Δt, is the probability of initial detection in that small time period, assuming the target has not yet been detected. Therefore, if T is the time of initial detection with pdf f(t) and cdf F(t), then

$$\gamma(t)\Delta t = \frac{P(t \le T \le t+\Delta t)}{P(T \ge t)} = \frac{f(t)\Delta t}{1 - F(t)},$$

or,

$$\gamma(t) = \frac{f(t)}{1 - F(t)}.$$

Since $\frac{dF(t)}{dt} = f(t)$, it is easily verified that a solution to this differential equation is

$$F(t) = 1 - \exp\left(-\int_0^t \gamma(u)du\right).$$

With this cdf for detection time T, the mean time of detection is

$$E[T] = \int_0^\infty \exp\left(-\int_0^t \gamma(u)du\right)dt.$$

For RS, the probability of target detection during time interval Δt, given no earlier detection, is the area searched during Δt, $2RV\Delta t$, divided by the total area, A. Applying the detection rate definition,

$$\gamma(t) = \frac{P(t \le T \le t+\Delta t)}{P(T \ge t)\,\Delta t} = \frac{2RV}{A}.$$

Therefore RS detection time, T, is an exponential random variable with mean equal to $1/\gamma = \frac{A}{2RV}$. [Ref. 2]

In ES the target is stationary so the maximum time spent searching is the time needed to cover the entire target region once, or $\frac{A}{2RV}$. Due to the fact that the target is at a uniformly distributed position somewhere on the target plane, the time to discover the target is a uniform random variable over $[0, \frac{A}{2RV}]$ and the mean time to detection is

$$E[T] = \frac{A}{4RV}.$$

For a more complete discussion see Washburn [Ref. 1:pp. 1-1 - 1-4].

Even though detection rates are generally not used to model ES, ES can be mathematically manipulated into a detection rate problem. In this model, the probability that the target has not yet been found is the total area, A, minus the area surveyed, 2RVt, divided by the total area,

$$P(t \geq T) = 1 - F(t) = \frac{A - 2RVt}{A},$$

consequently, after differentiation and algebraic manipulation, the pdf for T is

$$f(t) = \frac{2RV}{A}.$$

Therefore from the definition of detection rate,

$$\gamma(t) = \frac{2RV}{A - 2RVt}.$$

and the mean detection time is

$$E[T] = \int_0^{A/2RV} \exp\left(-\int_0^t \frac{2RV}{A - 2RVu}du\right)dt,$$

$$= \frac{A}{4RV}.$$

This agrees with the more conventional method used to derive ES.

The preceding examples suggest that the motion search problem could be solved as a detection rate problem. The trick is to determine the detection rate function, $\gamma(t)$.

C. AREA MOTION SEARCH DETECTION RATE FUNCTION

For search models with a target uniformly distributed over a fixed search area, the detection rate can be interpreted as

$$\gamma(t) = \frac{\text{rate of area search at t}}{\text{area where target can be located at t}}.$$

In AMS the area behind the searcher is swept free of targets. This area is known as the target free area (TFA) and is illustrated by Figure 1. The TFA has zero target density, while the rest of the search area has a uniform target density greater than zero. Therefore, the area where the target can be located at time t is the total search area minus the current TFA. This means the AMS detection rate is

$$\gamma(t) = \frac{\text{rate of area search at t}}{\text{search area - TFA(t)}}.$$

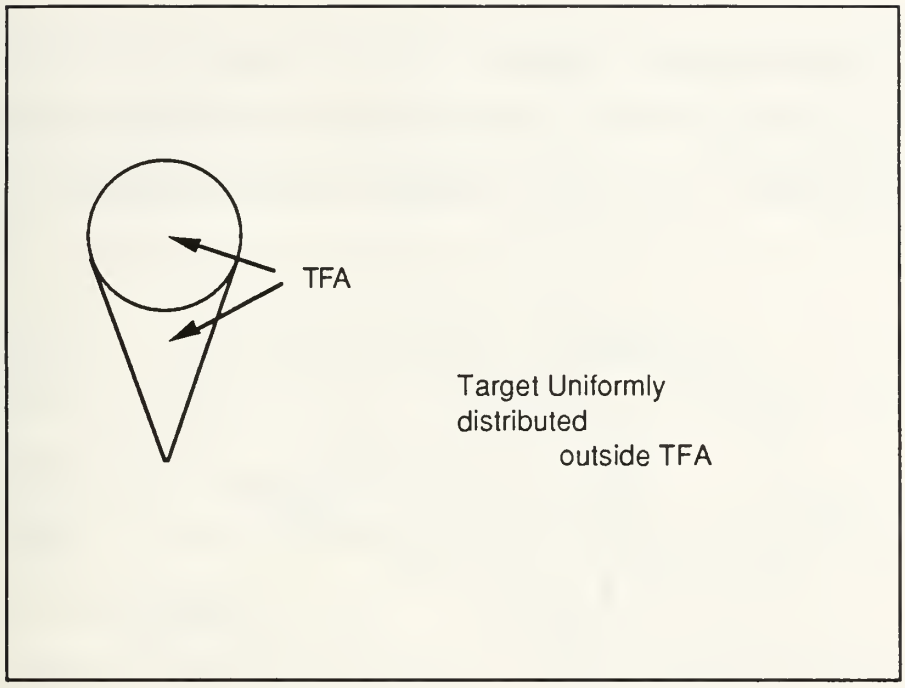

Figure 1. Searcher on Target Plane, with TFA

1. Cookie-Cutter Sensor Target Free Area

For a cookie-cutter sensor the TFA is an ice cream cone shaped region, as in Figure 2. This shape was developed by considering a target that just avoids detection, travelling perpendicular to the searcher's course. Two such targets on either side of the searcher meet at center of the searcher's path. In the meantime, the searcher has advanced some distance. These motions combine to define the TFA cone.

AMS starts as the searcher sweeps into the search area. Time zero occurs when the detection disk is first fully in the search area. As AMS progresses, the rest of the TFA is pulled into the search area.

This is illustrated in Figure 3. The cone portion of the TFA is attached to the detection disk at the point on the disk where the slope equals U/V, point a in Figure 2. This occurs at angle θ, where $\theta = \arctan(\frac{V}{U})$.

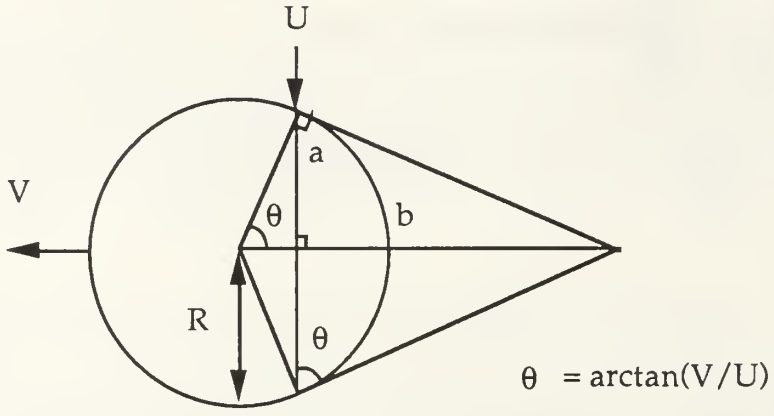

Figure 2. Target Free Area

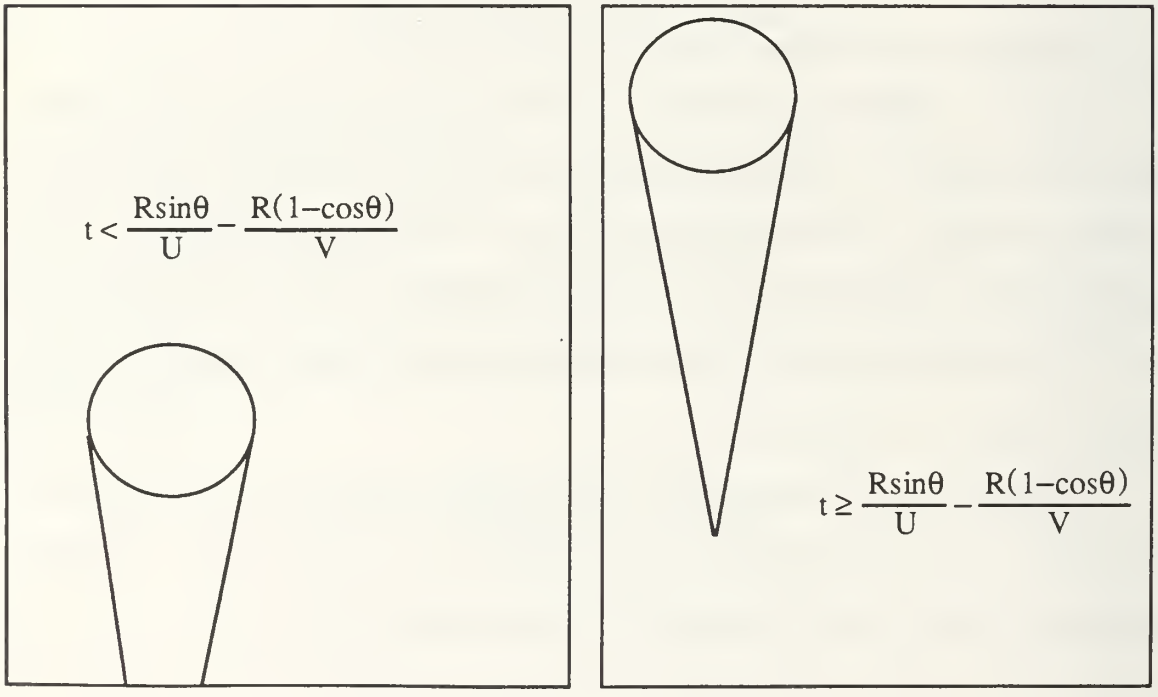

Figure 3. TFA Cone Development

The cone is fully pulled into the search area in the time it takes a target to travel to the center of the searcher's path from point a, $t = \frac{R\sin\theta}{U}$, minus the time the searcher requires to move from point a to point b, $\frac{R(1 - \cos\theta)}{V}$. Therefore, the mechanics of TFA development can be explained by two equations. One equation describing the sweeping of the full TFA into the search area, for time $t < \frac{R\sin\theta}{U} - \frac{R(1 - \cos\theta)}{V}$, and another equation after the entire TFA is in the search area.

Table 1 illustrates the areas of several geometric shapes used to derive the TFA equations.

Using the geometries derived in Table 1 the TFA equations for the ice cream cone shape are:

$$TFA(t)=\begin{cases} (\pi-\theta)R^2 + R^2\sin\theta\cos\theta - UV\left(t+\frac{R(1-\cos\theta)}{V}\right)^2 : t < \frac{R\sin\theta}{U} - \frac{R(1-\cos\theta)}{V} \\ \quad + 2VtR\sin\theta\left(t+\frac{R(1-\cos\theta)}{V}\right) \\ (\pi-\theta)R^2 + R^2\sin\theta\cos\theta + \frac{V}{U}R^2\sin\theta \qquad : t \geq \frac{R\sin\theta}{U} - \frac{R(1-\cos\theta)}{V} \end{cases}.$$

$$\text{where } \theta = \arctan\left(\frac{V}{U}\right).$$

These equations must incorporate one more contingency. Physically, the TFA can never be greater than the search area. As U approaches zero (as in ES) the TFA grows larger and the TFA equations will model a TFA that is larger than the search area. But, in reality, no more TFA will be drawn into the search area after the searcher has traversed the entire area once. The time require for a single searcher traverse is $\frac{A}{2RV}$.

Therefore, if $\frac{A}{2RV} < \frac{R\sin\theta}{U} - \frac{R(1 - \cos\theta)}{V}$ the first TFA equation is truncated at time $t = \frac{A}{2RV}$ and the TFA remains constant at that value for the rest of the search.

TABLE 1. TFA GEOMETRIES AND AREAS

Geometry	Area
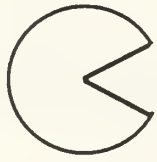	$(\pi - \theta)R^2$
	$R^2\sin\theta\cos\theta$
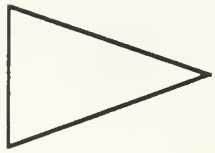	$(V/U)R^2\sin^2\theta$
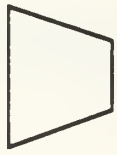	$2Vt(R\sin\theta) - UVt^2$

2. Line-sensor Target Free Area

In ES and RS the TFA is πR^2 when the searcher is motionless. Both classical ES and RS models ignore this area, implicitly assuming line-sensors rather than circular cookie-cutter sensors. The ice cream cone shape developed for the AMS model is based on a cookie-cutter sensor, consequently it will not ignore the πR^2 TFA and not simplify to the ES and RS

TFAs in the extremum. An AMS TFA based on a line-sensor will simplify to the actual ES and RS TFAs. Therefore, a line-sensor AMS TFA was developed and shaped as a triangle with width 2R and length RV/U. For a line-sensor,

$$TFA(t) = \begin{cases} 2RVt - VUt^2 & : \quad t < R/U \\ VR^2/U & : \quad t \geq R/U \end{cases}.$$

These equations are modified to reflect the possibility that the analytical TFA is larger than the search area, as in ES. This leads to

$$TFA(t) = \begin{cases} 2RVt - VUt^2 & : \quad t < \min\left[\frac{R}{U}, \frac{A}{2RV}\right] \\ \min\left[\frac{VR^2}{U}, A - \frac{A^2U}{4R^2V}\right] & : \quad t \geq \min\left[\frac{R}{U}, \frac{A}{2RV}\right] \end{cases}.$$

3. AMS Search Rate and Dynamic Enhancement

For many search models, the rate of area search equals the sweep rate. This is incorrect for AMS because it does not account for target motion. Target motion increases the rate of area search.

A model must be developed to dynamically enhance the searcher sweep rate with the target motion. **U** and **V** are velocity vectors of known length (V and U) and uniformly random direction. (Bold letters refer to vectors, plain letters refer to scalar length.) Therefore, the angle between **U** and **V**, θ, is uniformly distributed on $[0,2\pi)$. The vector addition of **U** and **V**, referred to as $\mathbf{V} \oplus \mathbf{U}$, also varies with θ. This is illustrated in Figure 4.

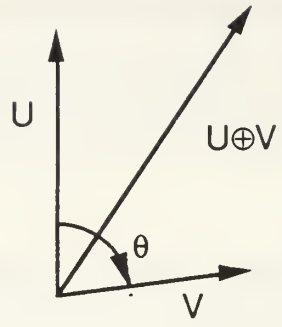

Figure 4. Vector Addition of V⊕U

The median of $|\mathbf{V}\oplus\mathbf{U}|$ is $\sqrt{V^2 + U^2}$ and occurs when **U** and **V** are at right angles. This is because θ is uniformly distributed over $(0,2\pi)$ and $|\mathbf{V}\oplus\mathbf{U}|$ is greater than $\sqrt{V^2 + U^2}$ when θ is $(-\pi/2,\pi/2)$ and less when θ is $(\pi/2,3\pi/2)$. The mean of $|\mathbf{V}\oplus\mathbf{U}|$ is given by Washburn as

$$E[|\mathbf{V}\oplus\mathbf{U}|] = 2(V+U)E(K)/\pi,$$

where

$$K = \frac{2\sqrt{U\,V}}{U + V}$$

and

$$E(K) = \int_0^{\pi/2} \sqrt{1 - K^2\sin^2\phi}\; d\phi.$$

E(K) is a complete elliptic integral of the second kind and cannot be explicitly evaluated, but is tabulated. Therefore $E[|\mathbf{V}\oplus\mathbf{U}|]$ can also be evaluated from tables, and ranges from 1.0 to 1.27 times the maximum of U or V. [Ref 1:pp. 6-1 - 6-4]

For purposes of model introduction, both dynamic enhancement models will notated by V⊕U.

4. AMS Line-sensor Detection Rate and Expected Detection Time

Using the definition from the beginning of the chapter, the AMS line-sensor detection rate is

$$\gamma(t) = \begin{cases} \dfrac{(V\oplus U)2R}{A-(2RVt-VUt^2)} & : \quad t < \min\left[\dfrac{R}{U}, \dfrac{A}{2RV}\right] \\ \max\left[\dfrac{(V\oplus U)2R}{A-R^2V/U}, \dfrac{(V\oplus U)8R^3V}{A^2U}\right] & : \quad t \geq \min\left[\dfrac{R}{U}, \dfrac{A}{2RV}\right] \end{cases}$$

Notice that if U or V equals zero these equations reduce to the ES and RS detection rates, respectively.

The cookie-cutter sensor detection rate is determined analogously. These detection rates can be plugged into the detection rate cdf to determine a closed form solution. The mean time to detection for the line-sensor model with $\frac{R}{U} < \frac{A}{2RV}$ can be determined by integrating 1 - cdf from zero to infinity,

$$E[T] = \int_0^{R/U} \exp\left[-\int_0^t \frac{(V\oplus U)(2R)}{A-2RVt+VUt^2}\,dt\right]dt + \int_{R/U}^{\infty}\left[\exp\left(-\int_0^{R/U}\frac{(V\oplus U)(2R)}{A-2RVt+VUt^2}\,dt - \int_{R/U}^{t}\frac{(V\oplus U)(2R)}{A-R^2\frac{V}{U}}\,dt\right)\right]dt.$$

Applying the integral formula

$$\int \frac{dx}{ax^2+bx+c} = \frac{2}{\sqrt{4ac-b^2}}\tan^{-1}\frac{2ax+b}{\sqrt{4ac-b^2}} \quad \text{(valid for } b^2 < 4ac\text{)}$$

where

$$a = VU$$

$$b = -2RV$$

$$c = A$$

yields the open form solution for expected detection time,

$$E[T] = \exp\left[\frac{2Z}{Bot}\tan^{-1}\left(\frac{-2RV}{Bot}\right)\right]\times$$

$$\left[\left(\frac{A - R^2V/U}{Z}\right) + \int_0^{R/U}\exp\left(\frac{-2Z}{Bot}\tan^{-1}\left(\frac{2VUt - 2RV}{Bot}\right)\right)dt\right]$$

where,

$$Bot = 2\sqrt{VUA - (RV)^2}$$

$$Z = (V \oplus U)2R.$$

D. EMBELLISHMENTS

The proposed AMS detection rates do not cover all possible scenarios. They can be embellished to reflect various possible occurrences.

A possibility exists that there is an area larger than the TFA, behind the searcher, with a target density less than that of the rest of the search area. This area will be called an effective target free area (ETFA). A TFA and a larger ETFA are illustrated in Figure 5.

Both edge effects of the search area and the fact that the target rarely travels directly perpendicular to the searcher can cause an ETFA to develop that is larger than the TFA. This leads to adding a constant of multiplication, R_u, to modify the TFA to create the longer ETFA. For example, if R_u equals two, the ETFA is twice the TFA. The resulting detection rate is

$$\gamma(t) = \begin{cases} \dfrac{(V \oplus U)2R}{A-(2RVt-VUt^2/R_u)} & : t < \min\left[\dfrac{R_u R}{U}, \dfrac{A}{2RV}\right] \\ \max\left[\dfrac{(V \oplus U)2R}{A - R_u R^2 V/U}, \dfrac{(V \oplus U)8R_u R^3 V}{A^2 U}\right] & : t \geq \min\left[\dfrac{R_u R}{U}, \dfrac{A}{2RV}\right] \end{cases}$$

Another problem arises because the AMS detection rates do not account for the searcher turning at corners. As the searcher turns, it sweeps out less area due to the rotation involved in turning. This means the sweep rate decreases. One way to account for this effect is to use an effective velocity for the searcher, V_{eff}, instead of the true velocity, V. V_{eff} will be less than V and will depend on the search pattern and search area geometry. V_{eff} is determined by dividing the area covered in one cycle of search by the time it takes to perform a search cycle and by the searcher's sweep width.

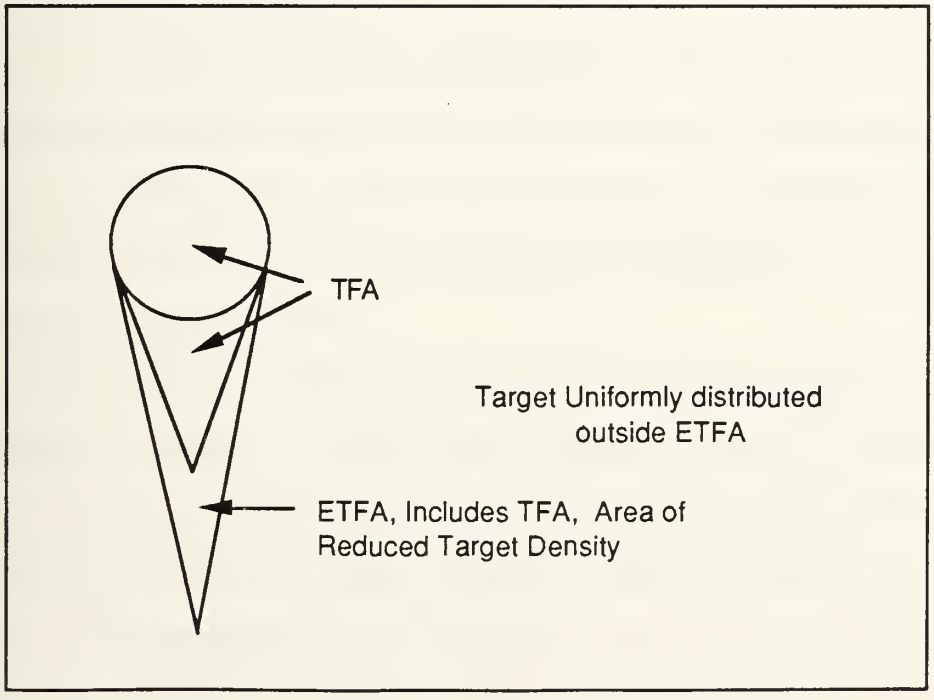

Figure 5. Searcher on Target Plane, with ETFA

Therefore, various permutations of the detection rate model must be investigated:

- Median versus mean dynamic enhancement, discussed in the previous section.
- V versus V_{eff} searcher velocities.
- Larger effective target free area versus the actual geometrically possible target free area.
- Line-sensor versus cookie-cutter sensor.

The resulting detection rate functions will be compared with the *Hounds and Hares* simulation results in the next chapter, Data Analysis, in an attempt to conclusively support one line-sensor detection rate model and check this model against the equivalent cookie-cutter model.

III. SIMULATION DEVELOPMENT AND VALIDATION

LT Richard L. Darden developed *Hounds and Hares* in the fall of 1991. The simulation was written in MODSIM II^{TM}, a modular, object-oriented simulating language. After adding a patrolling searcher and modifying the randomly moving target the model was empirically validated based on the RS and ES models. This chapter examines important aspects of the simulation's design. It explores search area design, searcher patrol parameters, the mechanics of the random target and validation of the simulation.

A. DESIGN CONSIDERATIONS

1. The Random Target

A truly random target has a position at one instant that is completely independent of the position at the next instant in time. It has the exact same probability of existing at one point as any other point. A stationary searcher would detect the target in the same average time regardless of the searcher's position on the fixed search area.

This condition is difficult to meet in a simulation and does not reflect reality. A target, in reality, has a continuous path. Therefore its position is not independent from one instant to the next instant. The random target in *Hounds and Hares* follows a continuous path. The target is generated at the beginning of a simulation run at a uniformly random position. It commences travel on a uniformly random course. When the target hits a search area boundary it is reflected by the diffuse reflection

process suggested by McNish in *Effects of Uniform Target Density on Random Targets* [Ref. 3:p. 43].

Diffuse reflection is based on Lambert's Law. Lambert's Law states that light reflects from a perfectly diffuse reflector according to $I_o\cos\theta$, where I_o is the incident light and θ, $(-\pi/2,\pi/2)$, is measured from the normal of the diffuse reflecting surface. [Ref. 4]

When a target hits an area boundary, the reflection angle is determined by selecting a standard uniform random variable, Z, and solving

$$\alpha = \arcsin(2Z - 1),$$

where α, the reflection angle, is measured from the normal of the boundary.

Specular and uniform reflection were also investigated.

The effect, on target randomness, of changing the target's course at random times, called course change times, was also explored. Course change times selected from exponential distributions were investigated.

Target randomness was investigated by placing a stationary searcher on a target plane containing a randomly moving target. The RS model predicted expected detection times equal to 100 (A=50, U=10, V=0, R=1.25). Table 2 illustrates various reflection characteristics and resulting average detection time confidence intervals.

Table 2 shows that both specular reflection with course change times and diffuse reflection with no course change times yield excellent random targets. The diffuse reflection method requires no predictive model to determine the best course change time, unlike the specular method. Therefore, in the simulation, the random target was programmed to follow diffuse reflection. Figure 6 shows the detection time cdf of both cases from

the data used for Table 2 superimposed on the ideal cdf. It shows how close targets using both reflection methods are to ideal random targets.

TABLE 2. TARGET CHARACTERISTIC COMPARISONS

Target Characteristics	95% Detection Time Confidence Interval
Uniform reflection- no random course changes	113-128
Specular reflection- no random course changes	167-190
Specular reflection- mean course change time = 5	96-109
Specular reflection mean course change time = 20	87-98
Diffuse reflection- no random course changes	91-104
Diffuse reflection- mean course change time = 20	104-118
Diffuse reflection- mean course change time = 5	96-109

Target density in the corners of the search area was slightly less than target density in the center of the search area. This is demonstrated by comparing the mean detection time for a stationary detector placed at different positions on the target plane. The RS model predicts an average detection time of 100 for the scenario illustrated on the contour plot of Figure 7. The contours show longer average detection times in the corners of the search area indicating lower target density in the corners.

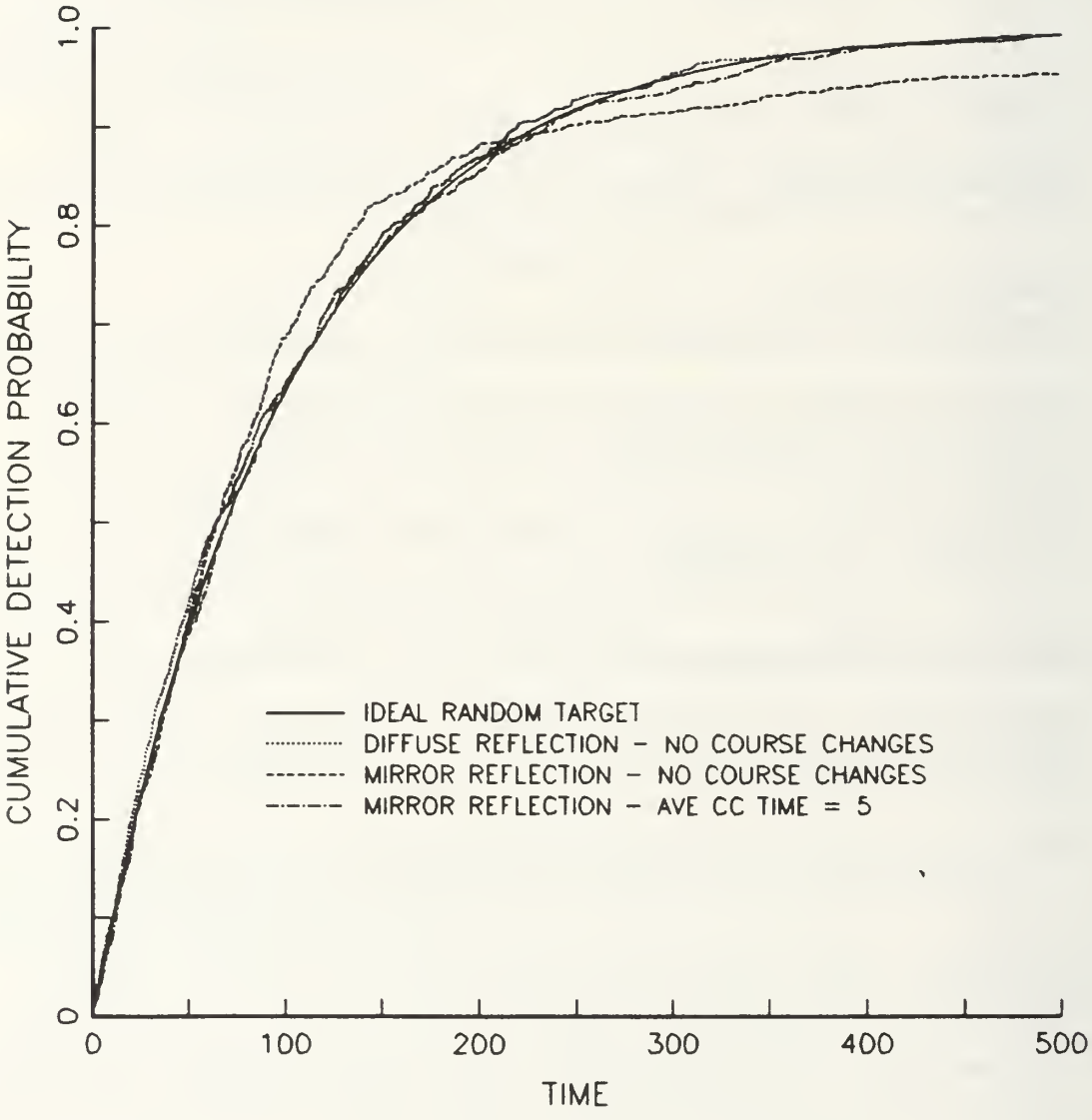

Figure 6. Cumulative Detection Probability vs Time for an RS Scenario with Different Target Characteristics

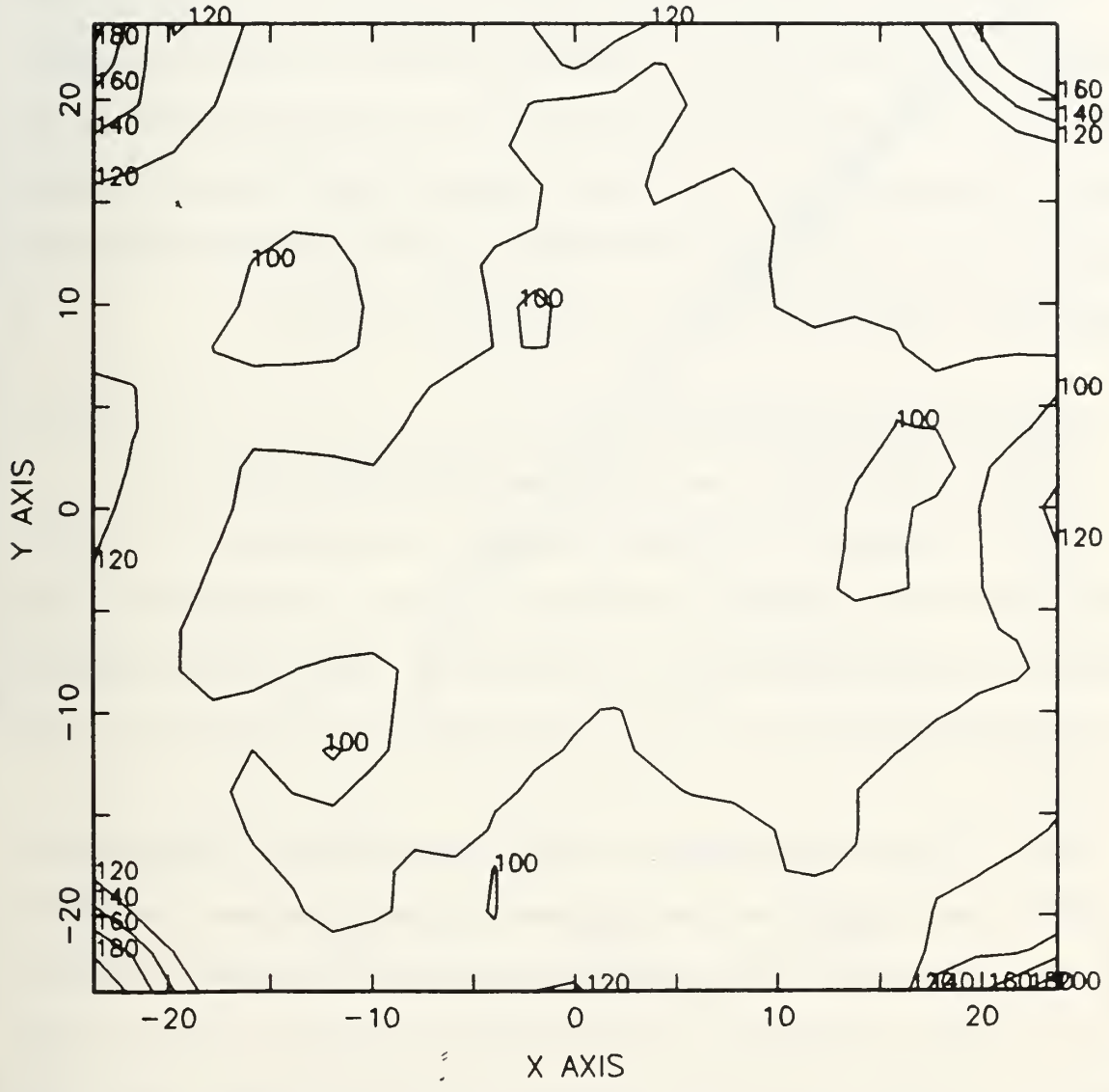

Figure 7. Average Detection Time Contour Plot for an RS Scenario with Predicted Detection Time = 100

2. The Patrolling Searcher and the Search Area

The search area was designed as a square and a ladder search was used as the searcher's patrol pattern. A ladder search consists of parallel paths offset by track spacing equal to twice the detection range [Ref. 5:p. 55]. Both the search area and the search pattern are typical of real world conditions.

Non-uniform target density, shown in Figure 7, can distort AMS results if the searcher spends an inordinate amount of time in low target density areas during many simulation runs. To overcome this problem, the searcher starts patrolling from random positions at the beginning of each simulation run. Consequently, the average target density seen by the searcher approaches a uniform density over the course of many runs.

B. SIMULATION VALIDATION

The ES and RS models were used to validate the simulation.

Figure 8 illustrates the detection times of 1000 simulation runs of RS, with predicted mean detection time 1300, plotted on a quantile-quantile plot against an exponential distribution with mean 1300. The results fall along the quantile-quantile plot's $x = y$ line. This validates the RS extreme of the simulation.

Figure 9 illustrates the results of 1000 simulation runs of ES plotted on a quantile-quantile against an ideal uniform distribution between 0 and 1332 time units. The range of this distribution was based on the effective velocity of the searcher, discussed in the Embellishments Section of the previous chapter. It was necessary to use V_{eff} because V itself predicted an upper limit of 1300 time units for the conditions of this model. Thus it did not reflect the

actual results. It is also intuitively correct to use V_{eff} in this case because V does not account for the turns the searcher makes in the ladder search. This quantile-quantile plot validates the ES extreme of the simulation.

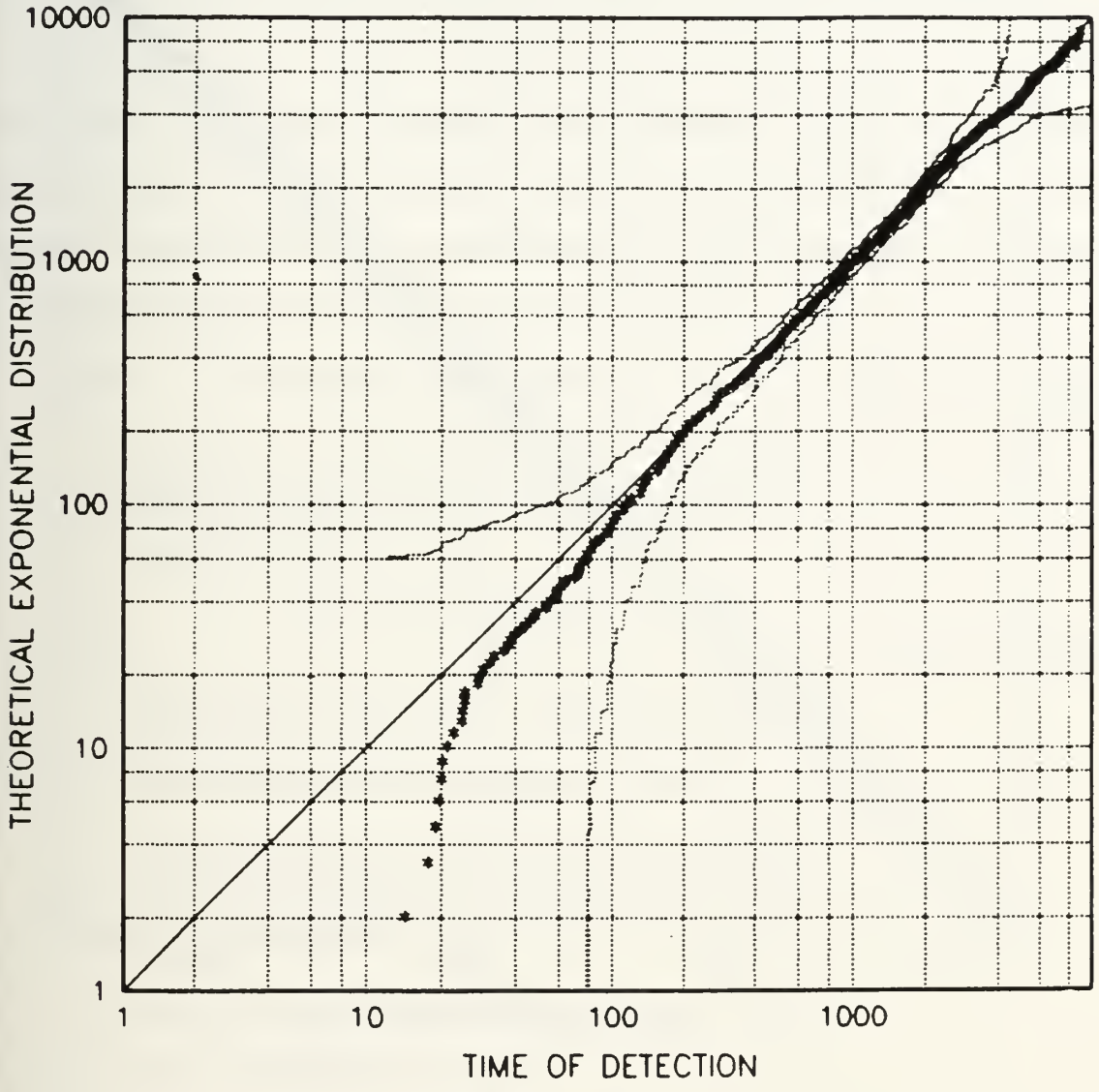

Figure 8. Quantile-Quantile Plot of Actual vs Ideal Detection Times for an RS Scenario

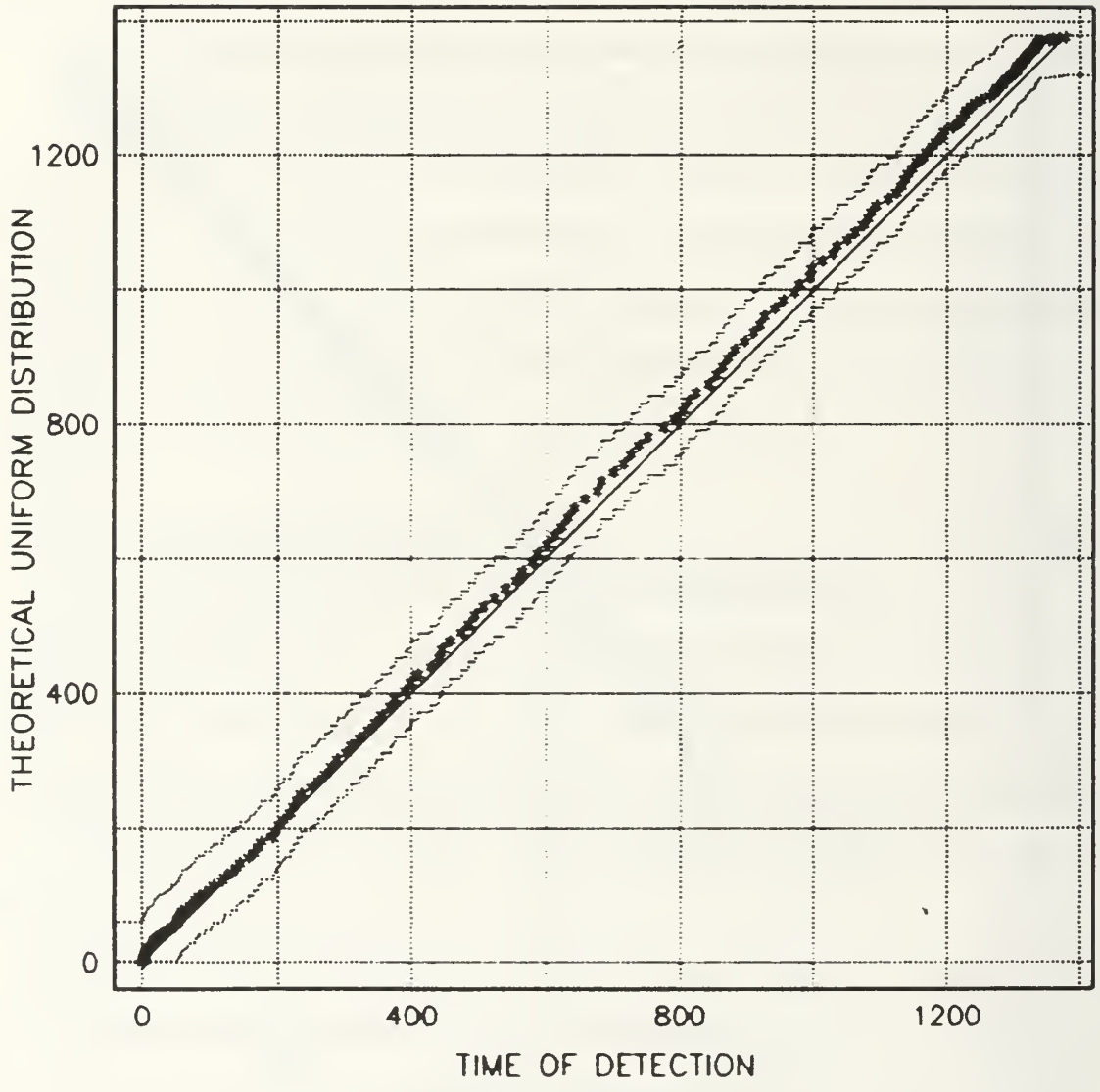

Figure 9. Quantile-Quantile Plot of Actual vs Ideal Detection Times for an ES Scenario

IV. DATA ANALYSIS

Data analysis was split into exploratory analysis and advanced analysis. Data analysis concentrated primarily on the line-sensor AMS model. During exploratory analysis 30 AMS scenarios were simulated to determine average detection times for each scenario. The simulation results were compared with detection time predictions from various line-sensor models AMS models. The initial findings were thoroughly explored in advanced analysis.

The following flowchart illustrates data analysis:

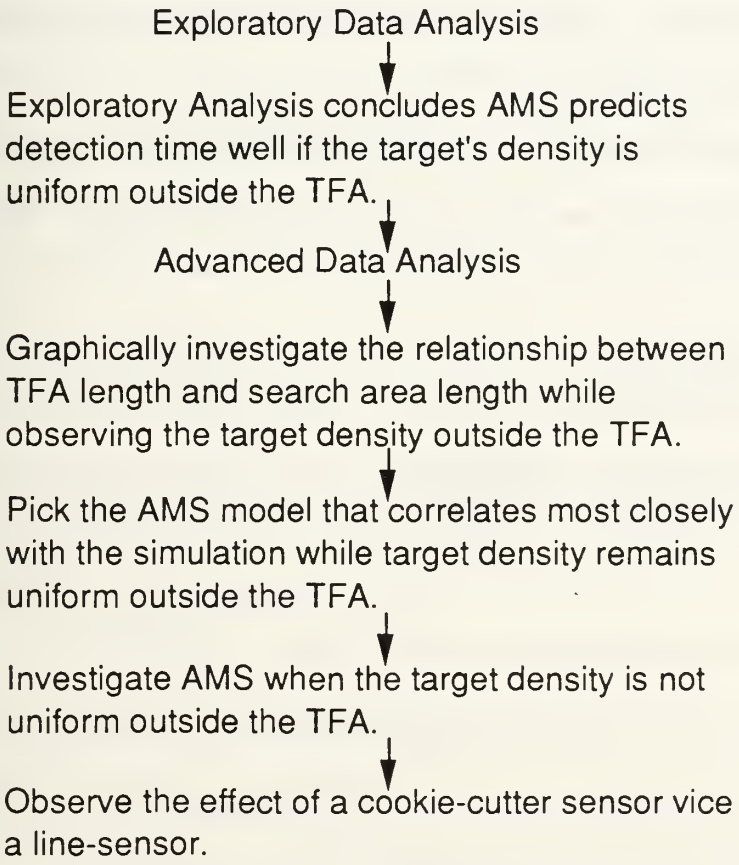
Exploratory Data Analysis
Exploratory Analysis concludes AMS predicts detection time well if the target's density is uniform outside the TFA.
Advanced Data Analysis
Graphically investigate the relationship between TFA length and search area length while observing the target density outside the TFA.
Pick the AMS model that correlates most closely with the simulation while target density remains uniform outside the TFA.
Investigate AMS when the target density is not uniform outside the TFA.
Observe the effect of a cookie-cutter sensor vice a line-sensor.

A. EXPLORATORY DATA ANALYSIS

During exploratory data analysis 30 different AMS scenarios were simulated to find a pattern between line-sensor model predictions and simulated detection times. The 30 cases were chosen based on a wide range of parameters. Search areas were squares with side lengths of 25, 50 and 100 units, target speeds were 1, 3, 5 and 10 units per time interval and searcher speeds were 5, 10, and 20 units per time intervals. Detection ranges were 1, 3, 5 and 10 units.

Each scenario was simulated to determine a 95% confidence interval for the mean detection time. The width of the confidence interval was less than 20 percent of the mean detection time.

Predicted detection times were evaluated by the basic line-sensor detection rate model using both methods of dynamic enhancement. The two detection rates are

$$\gamma(t) = \begin{cases} \dfrac{(V \oplus U)2R}{A-(2RVt-VUt^2)} & : \quad t < \min\left[\dfrac{R}{U}, \dfrac{A}{2RV}\right] \\ \max\left[\dfrac{(V \oplus U)2R}{A - R^2V/U}, \dfrac{(V \oplus U)8R^3V}{A^2U}\right] & : \quad t \geq \min\left[\dfrac{R}{U}, \dfrac{A}{2RV}\right] \end{cases}$$

$$\text{median dynamic enhancement model: } V \oplus U = \sqrt{V^2 + U^2}$$

$$\text{mean dynamic enhancement model: } V \oplus U = E[\,|\,\mathbf{V} \oplus \mathbf{U}\,|\,].$$

The predicted times from both models were compared with the center of the detection time confidence intervals in an effort to find a relationship.

A pattern emerged. Predicted and simulated detection times were similar if the time required for the searcher to traverse a length of the search area was at least five times greater than the time necessary for a target to travel to the center of the searcher's path from the edge of the searcher's path. Another way to look at this ratio is the length of the search area, L, (L is the square root of A for a square search area) compared to the length of the target free cone, RV/U. In symbolic terms, if

$$\frac{LU}{RV} \geq 5$$

then predicted and simulated detection times matched well.

It should be noted that if U equals zero this ratio equals zero and AMS simplifies to ES. Predicted and simulated detection times also match well in this situation. Data analysis approached AMS primarily from the RS extreme towards the ES extreme.

This conclusion makes intuitive sense. The greater the ratio $\frac{LU}{RV}$ is, the the smaller the TFA is in comparison with the search area. Therefore, it is less likely that the TFA interacts with search area edges. The embellishments to the basic model, ETFA and effective searcher velocity, are largely a result of edge effects. Consequently, embellishments to the model are unimportant if the ratio $\frac{LU}{RV}$ is greater than five.

B. ADVANCED DATA ANALYSIS

Exploratory data suggested that if,

$$\frac{LU}{RV} \geq 5,$$

then either dynamic enhancement AMS line-sensor model provides accurate forecasts of detection time. If the $\frac{LU}{RV}$ ratio is below five other factors affect the results.

1. ETFA versus TFA

The accuracy of the basic model when $\frac{LU}{RV}$ is greater than five leads to the conclusion that the ETFA approaches the TFA for these scenarios. To investigate, a scenario with $\frac{LU}{RV}$ greater than five was selected. The scenario was simulated many times (~1000) while the searcher was started in a corner of the search area. Each simulation was stopped when the searcher reached the center of the search area. The position of undetected targets was plotted. The geometric TFA was overlaid. Figure 10 illustrates for a scenario with a ratio of 8.33. The geometric TFA is drawn and the target density is roughly constant outside the TFA. The ETFA equals the TFA. These results are consistent with results from other scenarios with ratios greater than five.

The results of Figure 10 lead to an interesting question. Is the ETFA > TFA for low ratios? Graphs created by the previous method indicate yes. One of the more striking is for a scenario with a ratio equal to 1.67, illustrated in Figure 11. The density of targets outside the geometric TFA in this graph is not uniform. There is a lower density swath that corresponds to an ETFA longer than TFA. This effect disappears as the $\frac{LU}{RV}$ ratio is increased.

2. The Most Accurate Line-Sensor AMS Model

200 simulation scenarios with $\frac{LU}{RV}$ greater than five were investigated. They were divided into ten groups of 20 scenarios with $\frac{LU}{RV}$ = 10,20,...,100. The cases were determined by randomly selecting A between 25

and 100, U and V between 1 and 20, setting the ratio $\frac{LU}{RV}$ constant and solving for R.

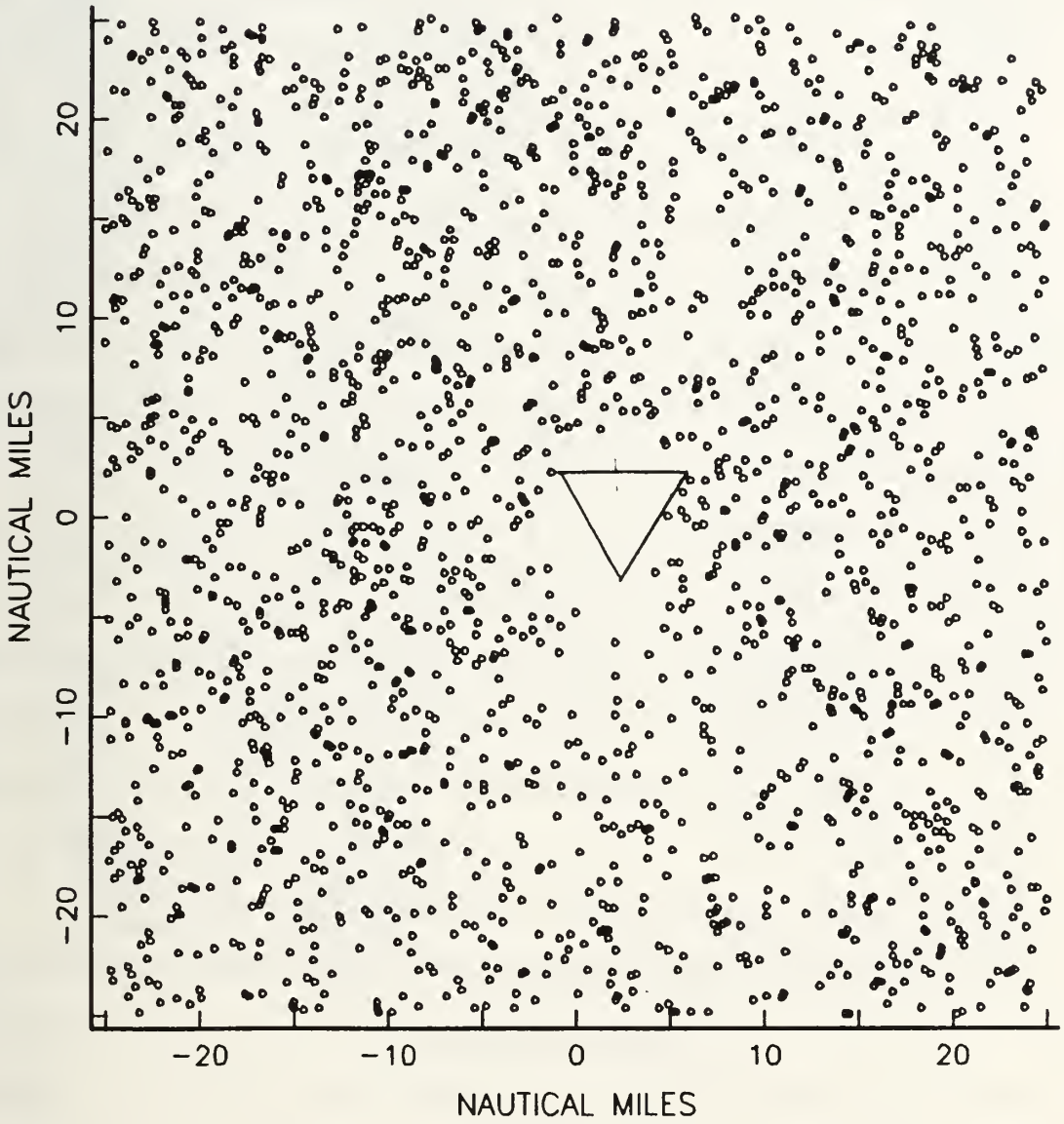

Figure 10. Target Density and TFA for $\frac{LU}{RV} = 8.33$

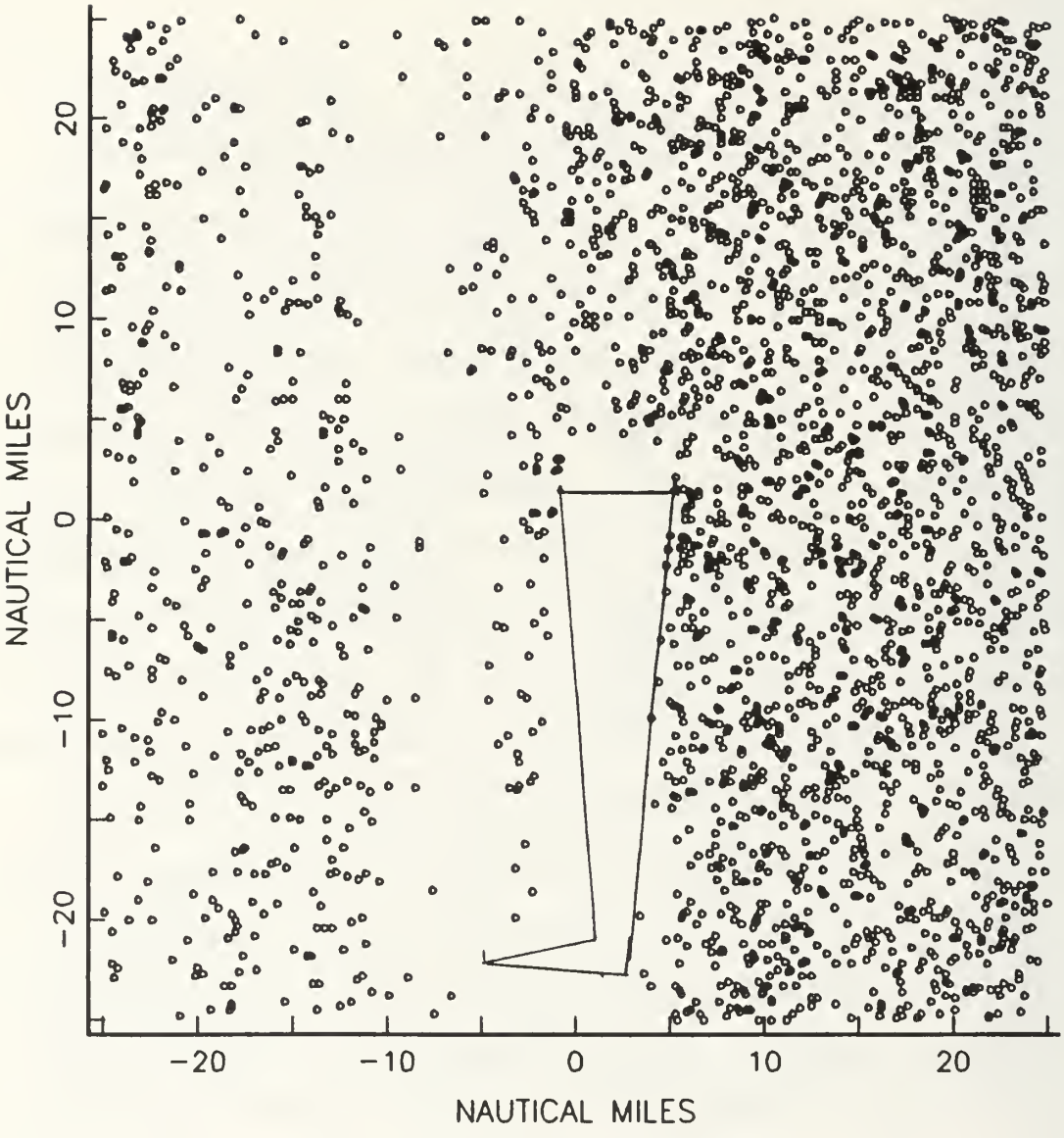

Figure 11. Target Density and TFA for $\frac{LU}{RV} = 1.67$

The simulation results were compared with four detection times predicted by four different line-sensor detection rate models consisting of permutations of the two dynamic enhancement models and the searcher true and effective velocities. Symbolically, $V \oplus U$ in the standard line-sensor detection rate formula was replaced by

$$E[|\mathbf{V} \oplus \mathbf{U}|], \quad E[|\mathbf{V}_{\mathbf{eff}} \oplus \mathbf{U}|], \quad \sqrt{V^2 + U^2} \text{ and } \sqrt{V_{eff}^2 + U^2}.$$

The results were compared by determining the relative error between each predicted and simulated detection time. The relative error of each prediction was averaged into an average relative error for each predictive model. The results are illustrated by the box plot in Figure 12.

The mean dynamic enhancement ($V \oplus U = E[|\mathbf{V} \oplus \mathbf{U}|]$) detection rate model provided the least average error at the 2% significance level according to Fisher's least significant difference method. [Ref. 6] This model's predictions had an average percent error between 3.8% and 4.8% at the 95% confidence level. Figure 13 illustrates the results of this model plotted against actual detection time. Figure 14 plots the residuals of Figure 13.

3. Effective Searcher Speed

The effective searcher speed embellishment, V_{eff}, is designed to account for a searcher sweeping less area in a turn, leading momentarily to a reduced detection rate. It is interesting to examine why the actual searcher speed, V, provides a better model of the simulation than V_{eff}, as shown in Figure 12. One reason may be that V provides a better detection rate for the great majority of search time so a V_{eff} based detection rate is unnecessary. The physical *Hounds and Hares* simulation characteristics might also cause

this effect. The reduced target density at the edges of the simulation search area may already compensate for the turning searcher making a V_{eff} correction redundant.

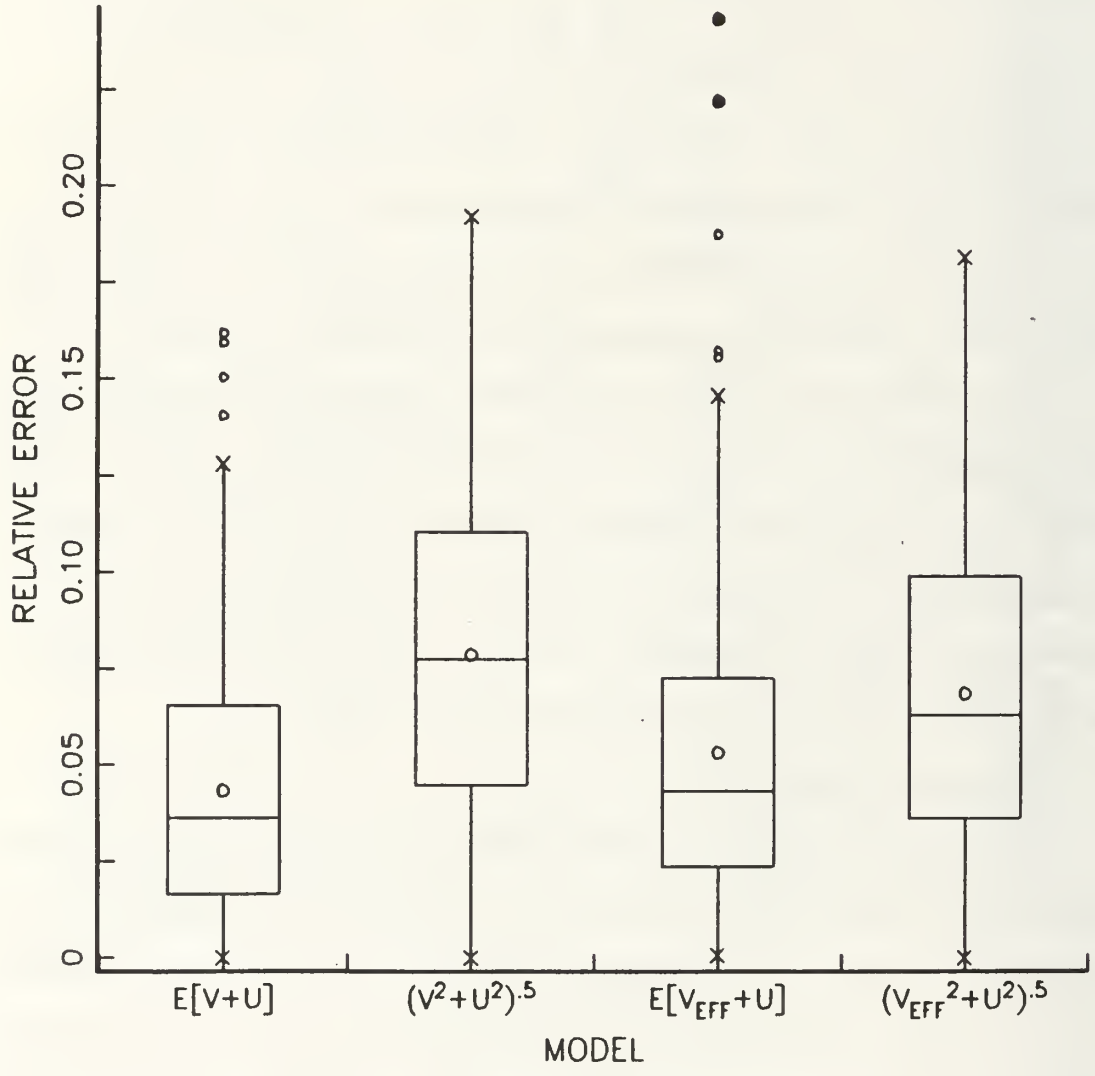

Figure 12. Box Plot of Relative Error between Simulation and AMS Model Predictions

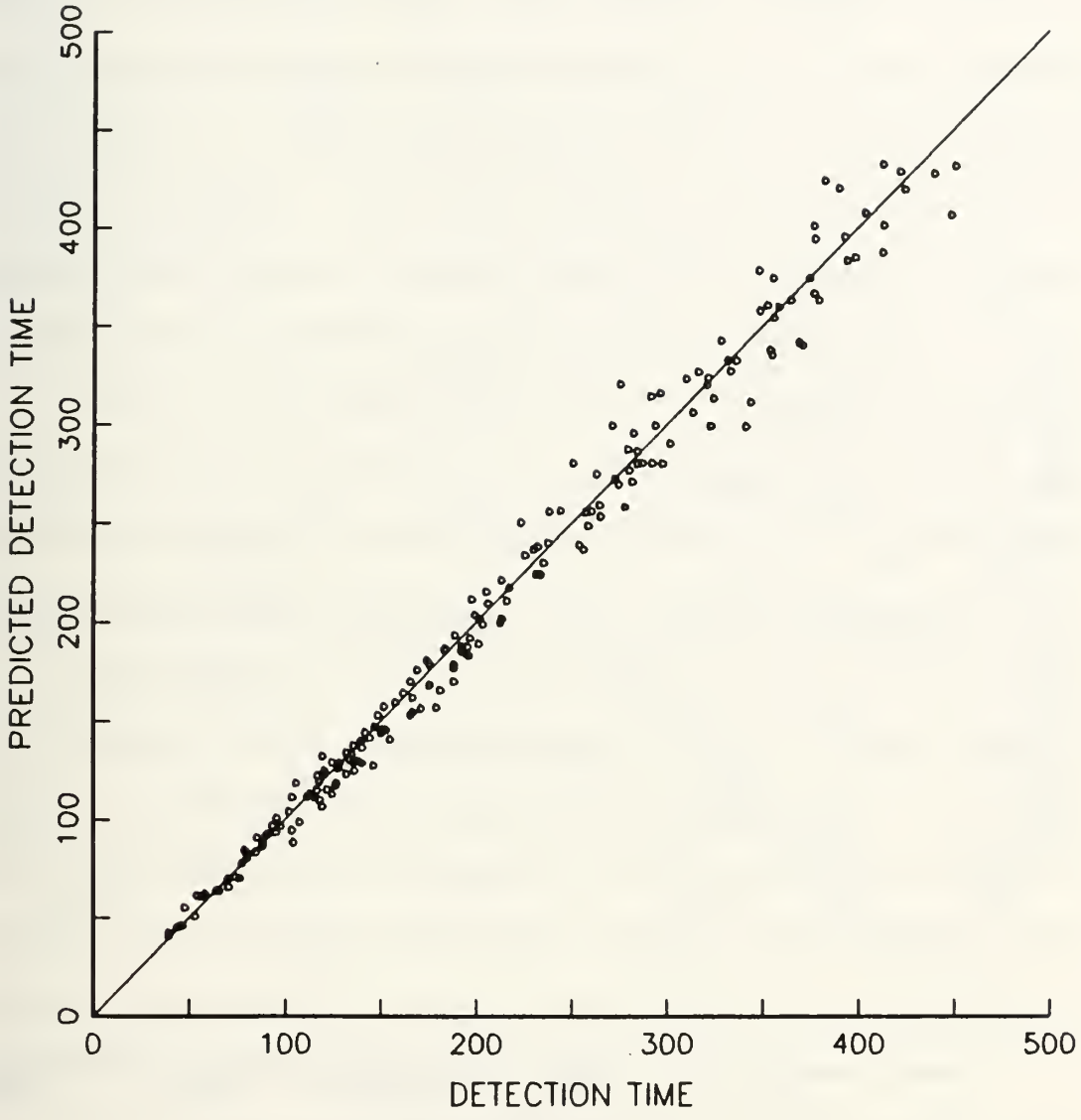

Figure 13. Predicted vs Simulated Detection Times for Scenarios with $\frac{LU}{RV} > 10$

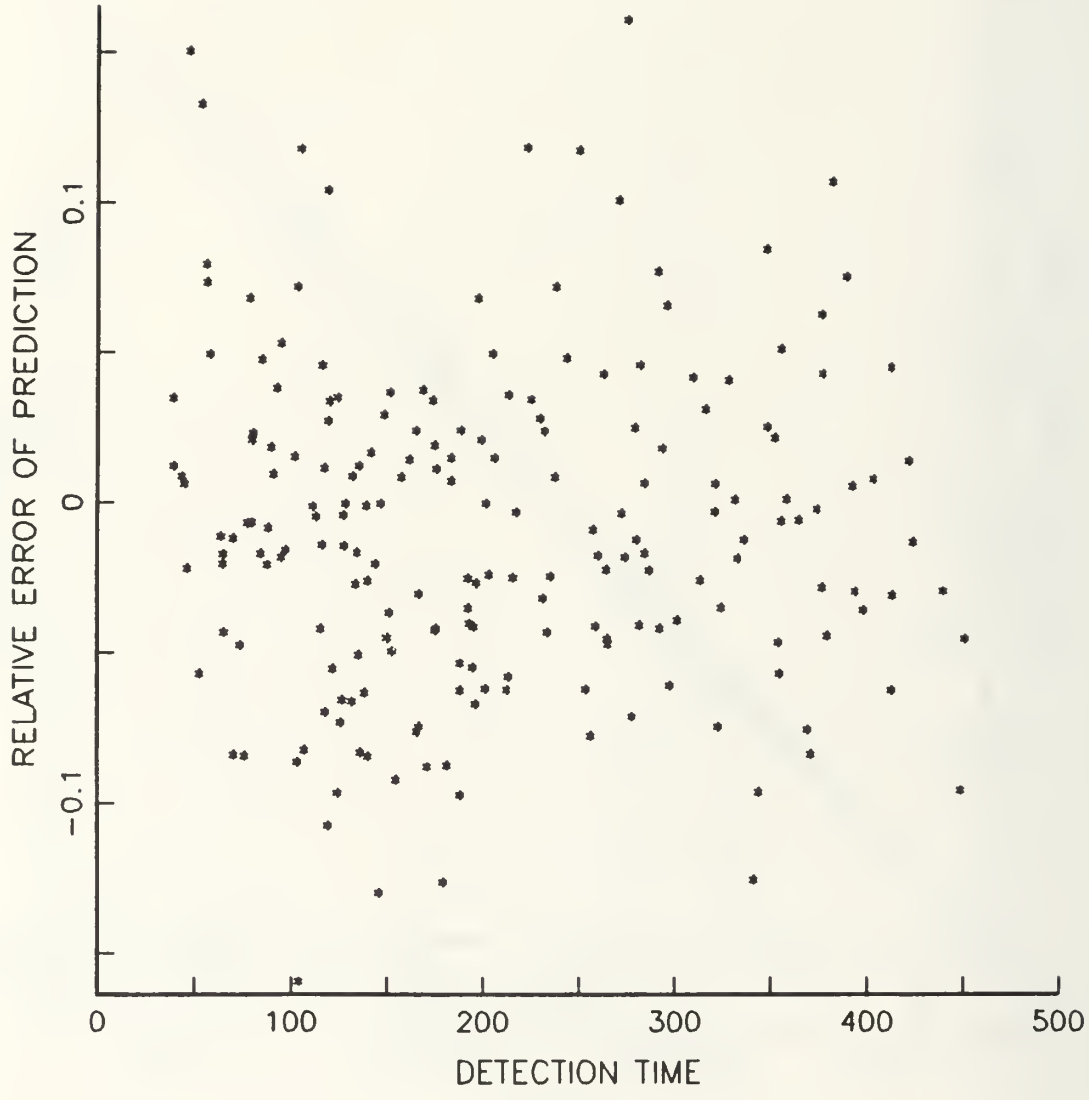

Figure 14. Error between Predicted and Simulated Detection Times for Scenarios with $\frac{LU}{RV} > 10$

4. ETFA versus TFA for Small $\frac{LU}{RV}$ Scenarios.

The basic AMS model does not successfully predict detection times for scenarios with small $\frac{LU}{RV}$ ratios. This is illustrated by Figures 15 and 16. In Figure 15 simulated detection times are plotted against predicted detection times for scenarios with $\frac{LU}{RV}$ ratios between one and five. Figure 16 is a plot of the resulting residuals. The poor correlation between predicted and simulated detection times is the result of large TFAs interacting with search area edges to create non-uniform target densities outside the TFAs.

Scenarios with smaller $\frac{LU}{RV}$ ratios were investigated to see if the ETFA embellishment helps predict accurate detection times. 50 random scenarios were developed for each $\frac{LU}{RV}$ ratio in the set (1,2,...,10). The detection rate model with the ETFA embellishment was applied to the scenarios.

Each scenario was examined with ETFAs that were multiples of the TFA. A sensitivity range was determined for the TFA multiples based on average error between predicted and simulated detection times. The valley in Figure 17 shows the ranges of multiples, R_u, that yield the least average error for each $\frac{LU}{RV}$ scenario. Figure 17 shows that as the $\frac{LU}{RV}$ ratio gets smaller, down to about one, the optimal R_u becomes greater. This is due to the increasing interaction of the TFA with search area edges.

Figure 17 shows that for large $\frac{LU}{RV}$ ratios, the TFA is relatively small, and the model is less sensitive to increasing ETFA. In fact, the results in the Figure 17 show that ETFA effects can be ignored for ratios as low as $\frac{LU}{RV} \geq 5$.

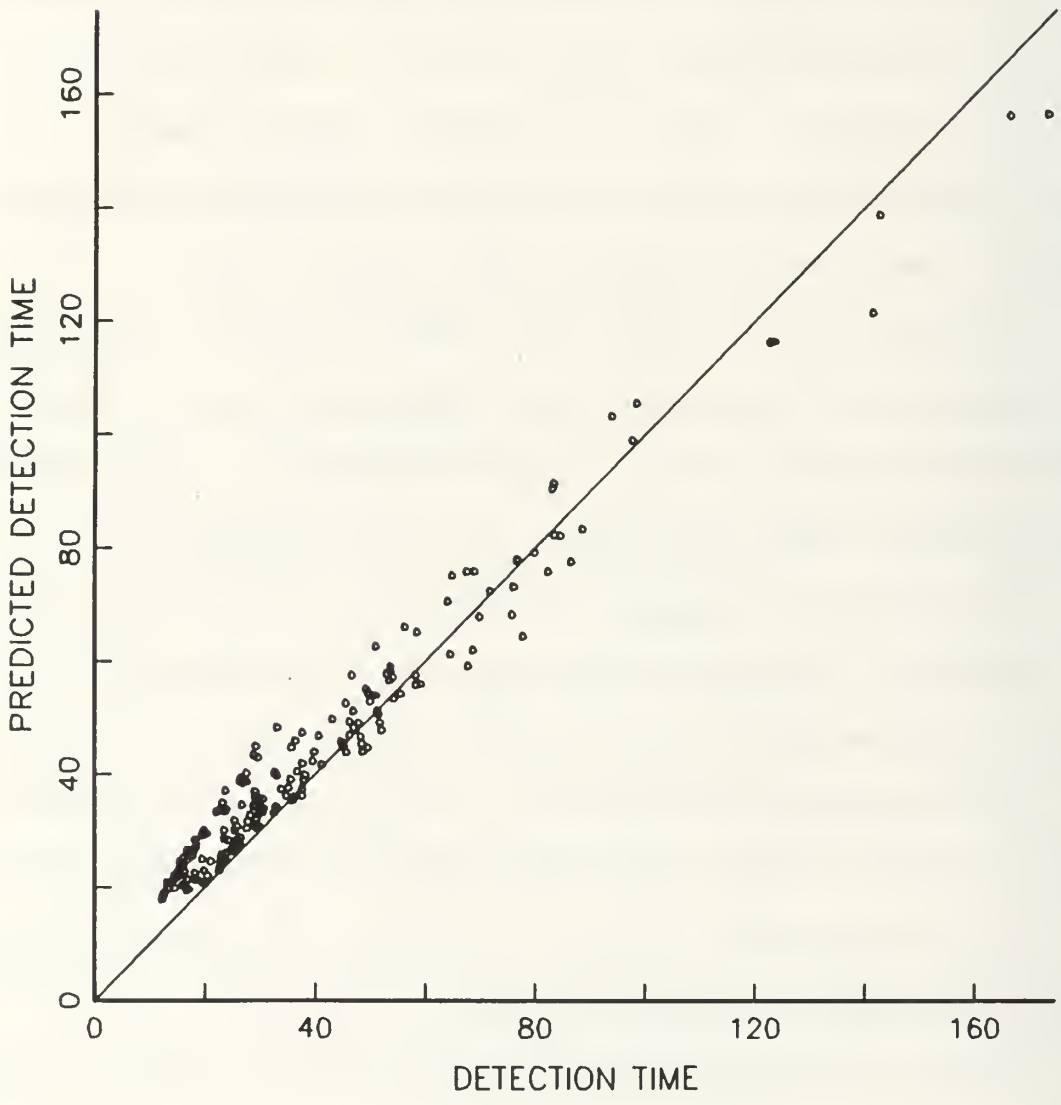

Figure 15. Predicted vs Simulated Detection Times for Scenarios with $\frac{LU}{RV} < 10$

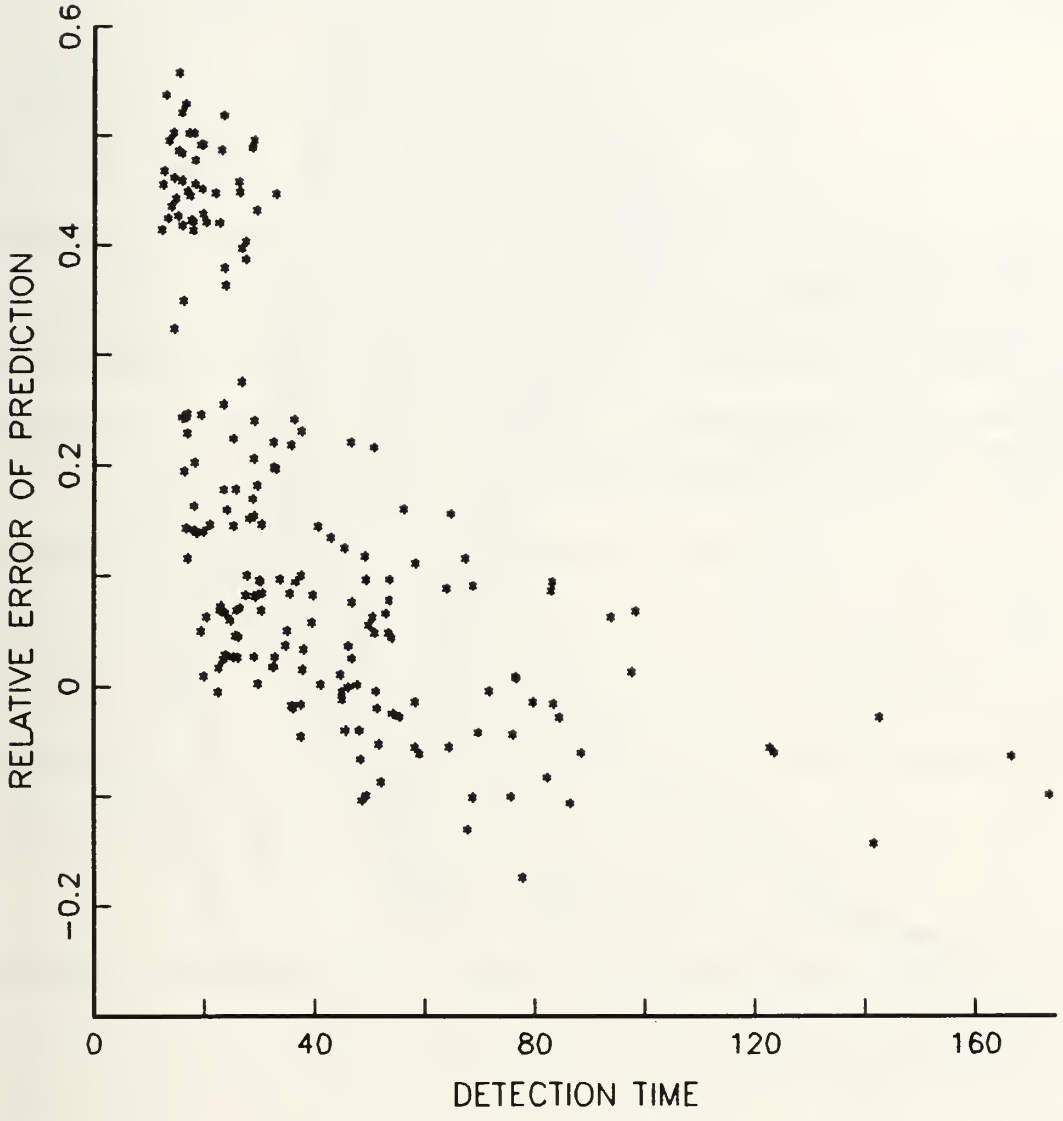

Figure 16. Error betweeen Predicted and Simulated Detection Times for Scenarios with $\frac{LU}{RV} < 10$

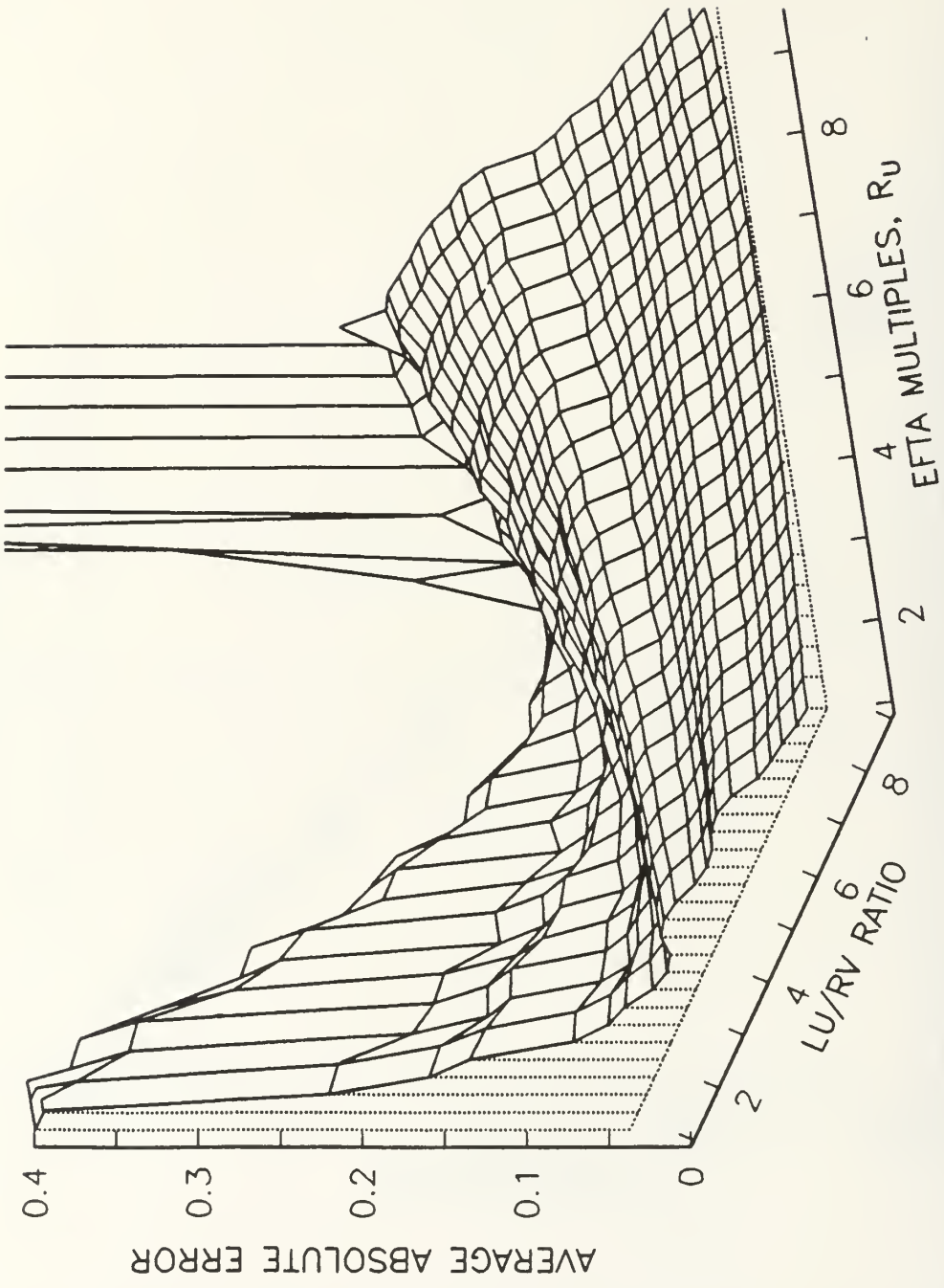

Figure 17. 3-D Contour Plot of Average Error vs ETFA Multiples

Figures 18 and 19 plot the same scenarios as Figures 15 and 16, while applying an ETFA correction to the AMS model. The results are vastly improved.

In order to examine AMS when $\frac{LU}{RV} <$ one, 50 random scenarios were simulated for each $\frac{LU}{RV}$ ratio in the set (0.2,0.3,0.5,0.7,0.8).

The results of scenarios with ratios below 0.8 are nearly indistinguishable from ES predictions (as if U = 0). These scenarios reflect the ES extreme of AMS because the target has little probability of crossing the searcher's long tail. In fact, an AMS prediction with an ETFA embellishment is only slightly better than an ES prediction in this region.

An ETFA embellishment was applied to these scenarios. Figure 20 interpolates and plots the results. Figure 20 shows that the optimal R_u decreases as $\frac{LU}{RV}$ decreases below one because these scenarios approach exhaustive search. The optimal R_u forces the ETFA to equal the TFA for the equivalent ES scenario with U equal to zero. The optimal Ru and the TFA tend to follow the rough relationship

$$(TFA_{true}) \times (R_u) \sim TFA_{ES} .$$

As TFA_{true} becomes larger, R_u becomes smaller to maintain constant TFA_{ES}.

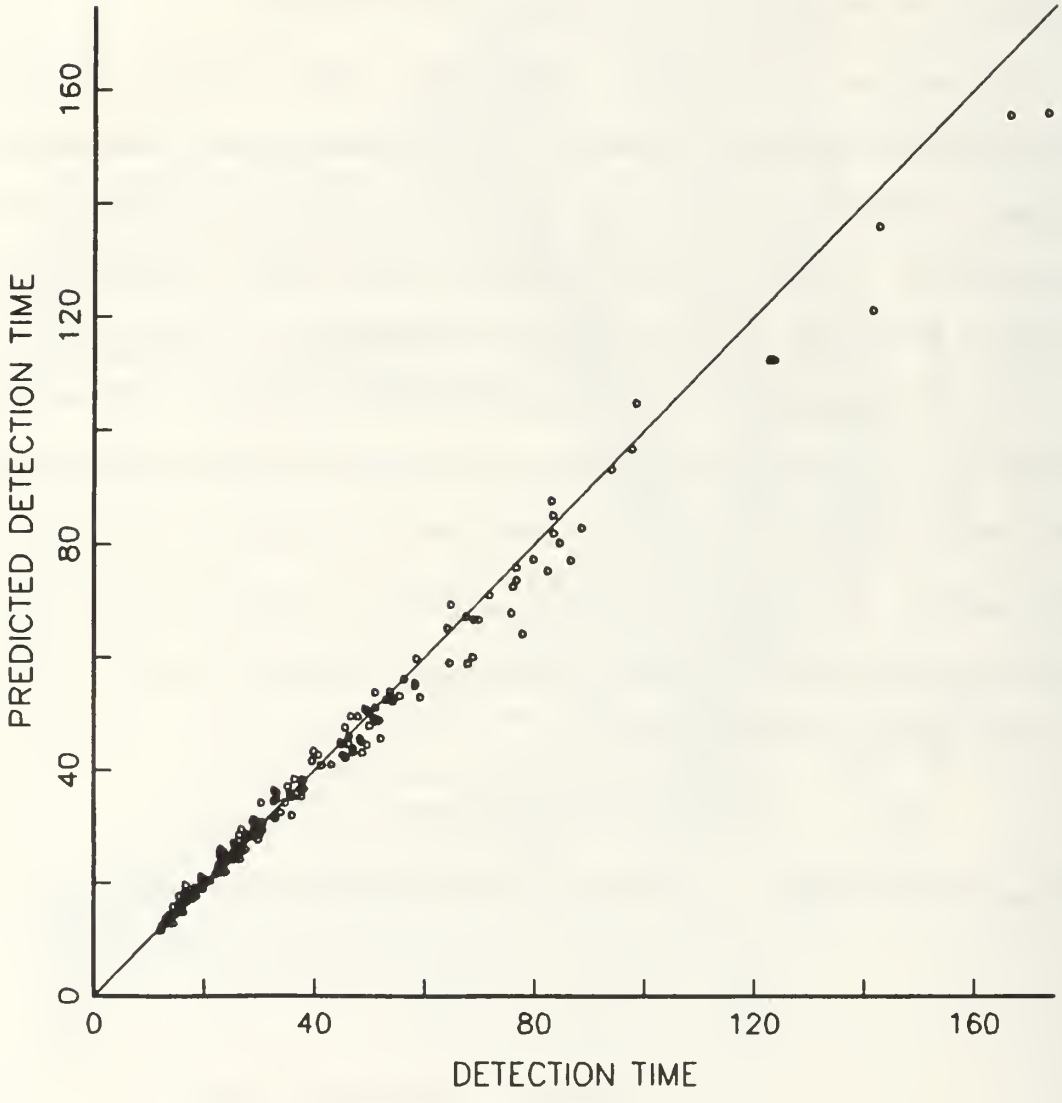

Figure 18. Corrected Predicted vs Simulated Detection Times for Scenarios with $\frac{LU}{RV} < 10$

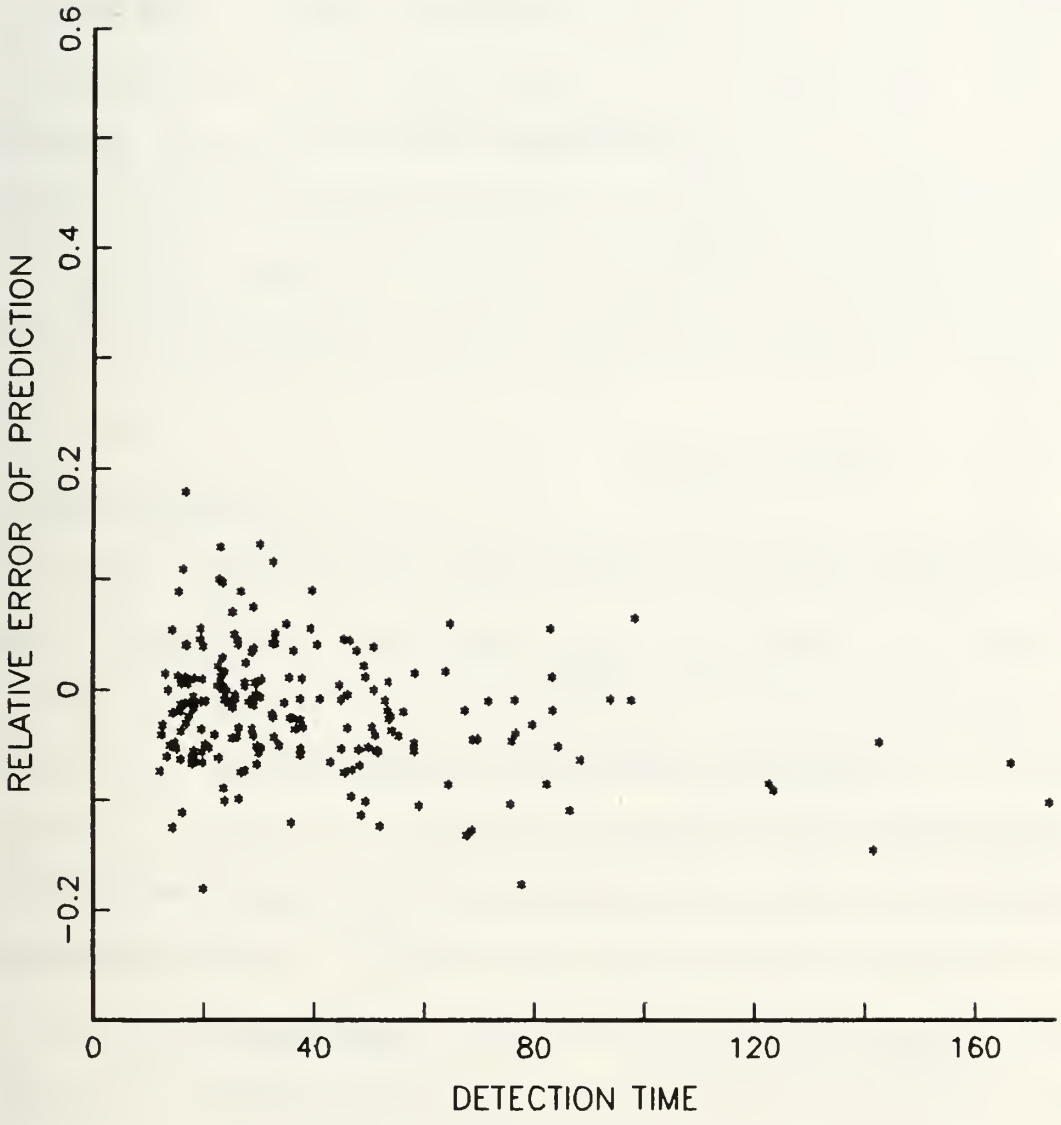

Figure 19. Error between Corrected Predicted and Simulated Detection Times for Scenarios with $\frac{LU}{RV} < 10$

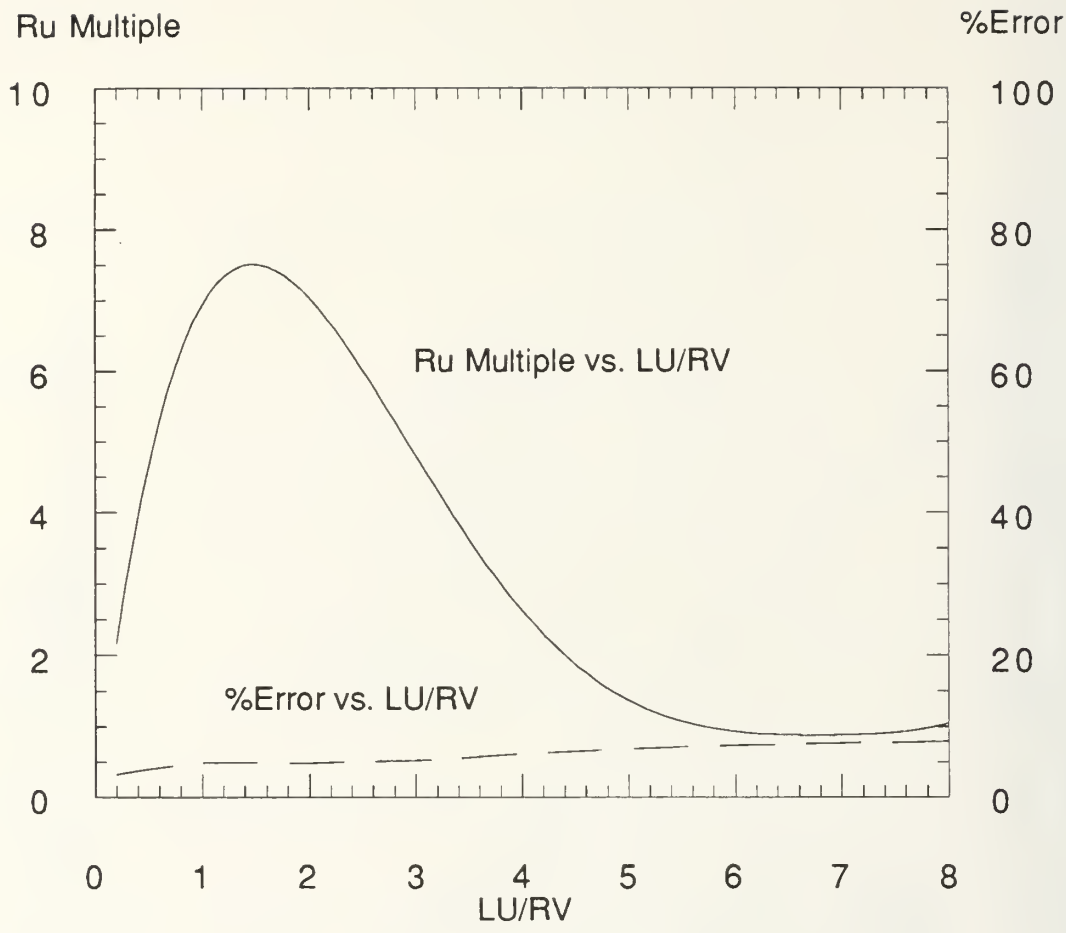

Figure 20. R_u and Error vs. LU/RV ratio

5. Line-sensor versus Cookie-Cutter Sensor

The results of the cookie-cutter sensor model were indistinguishable from the line sensor model for ratios as low as $\frac{LU}{RV} \geq 5$. This is expected because in higher ratio scenarios the model loses sensitivity to TFA, as illustrated in Figure 17. Therefore the slightly larger shape of the cookie-cutter TFA will not affect the results. Differences between the models in lower $\frac{LU}{RV}$ regions are visible, requiring different ETFA corrections for the two models.

V. CONCLUSIONS AND RECOMMENDATIONS

This thesis attempts to shed light on an interesting area of search theory, area motion search. While investigating this phenomenon, many subtopics were touched upon: the characteristics of a random target and the relationship of edge effects on search models are just a few. Many conclusions can be drawn from this thesis, but all must be treated skeptically as they are only as good as the supporting simulation. In short, this is a dynamic area of operations research that could benefit from much more study.

A. CONCLUSIONS

The area motion search problem can be treated as a detection rate problem. Line-sensor and cookie-cutter sensor detection rate models both predict area motion search well when the target is uniformly distributed over the search area. The line-sensor area motion search detection rate reduces to the classical exhaustive search detection rate and random search detection rate when the target and searcher velocities are zero, respectively. The line-sensor detection rate is

$$\gamma(t) = \begin{cases} \dfrac{(V \oplus U)2R}{A-(2RVt-VUt^2)} & : \quad t < \min\left[\dfrac{R}{U}, \dfrac{A}{2RV}\right] \\ \max\left[\dfrac{(V \oplus U)2R}{A - R^2V/U}, \dfrac{(V \oplus U)8R^3V}{A^2U}\right] & : \quad t \geq \min\left[\dfrac{R}{U}, \dfrac{A}{2RV}\right] \end{cases}$$

A = search area, V = searcher velocity, U = target velocity, R = detection range

If the target is bounded by the search area, edge effects can prevent uniform target distribution over this area. Edge effects can be ignored for a square search area when the length of the search area is on the order of five times greater than the length of the target free area, or

$$\frac{LU}{RV} \geq 5, \quad L = \text{length of a search area edge.}$$

When edge effects cannot be ignored, the line-sensor detection rate can be modified by expanding the target free area to equal an effective target free area to accurately predict average detection times. The effective target free area accounts for reductions in target density in certain parts of the search area due to the interaction of the true target free area with the edges of the search area.

To expand the target free area, the factor R_u was introduced into the existing line-sensor detection rate to create a new detection rate,

$$\gamma(t) = \begin{cases} \dfrac{(V \oplus U)2R}{A-(2RVt-VUt^2/R_u)} & : t < \min\left[\dfrac{R_uR}{U}, \dfrac{A}{2RV}\right] \\ \max\left[\dfrac{(V \oplus U)2R}{A - R_uR^2V/U}, \dfrac{(V \oplus U)8R_uR^3V}{A^2U}\right] & : t \geq \min\left[\dfrac{R_uR}{U}, \dfrac{A}{2RV}\right] \end{cases}$$

For example, if R_u equals two, the effective target free area is twice the geometric target free area.

Figure 20 illustrates optimum R_u multiples versus $\frac{LU}{RV}$ for a square search area and a ladder search pattern. Figure 20 shows R_u increasing as $\frac{LU}{RV}$ increases from zero to one, R_u peaking near $\frac{LU}{RV}$ = one and R_u decreasing as $\frac{LU}{RV}$ increases beyond one.

Ru decreases as $\frac{LU}{RV}$ increases above one because the target free area becomes smaller in relation to the search area. This makes edge effects less prominent, and smaller effective target free areas are required.

R_u increases as $\frac{LU}{RV}$ increases from zero to one, because these scenarios approach exhaustive search. The optimal R_u multiple forces the effective target free area to roughly equal the target free area for the equivalent exhaustive search scenario (target velocity equals zero), according to

$$(\text{target free area}_{true}) \times (R_u) \sim \text{target free area}_{\text{exhaustive search}}.$$

Therefore, as target free area_{true} becomes smaller, R_u becomes larger to maintain constant target free $\text{area}_{\text{exhaustive search}}$.

B. RECOMMENDATIONS FOR FURTHER RESEARCH

This thesis suggests many areas for further research, including:

- Determine the optimal real world search pattern for a searcher in AMS.
- Attempt to duplicate the results on different search area geometries with different search patterns.
- Investigate the best random target characteristics for simulation.
- Investigate edge effects more closely.
- Investigate the affects of introducing a smart target to the model.
- Attempt to validate the model in sea tests.
- Introduce the area motion search into low-fidelity combat models.

REFERENCES

1. Washburn, Alan R., *Search and Detection*, 2nd ed., ORSA Books, 1989.

2. Koopman, Bernard O., *Search and Screening General Principles with Historical Applications*, pp 71-74, Pergamon Press, 1980.

3. McNish, Michael J., *Effects of Uniform Target Density on Random Search*, Master's Thesis, Naval Postgraduate School, Monterey, California, September 1987.

4. Besancon, Robert M., editor, *The Encyclopedia of Physics*, 3rd ed., pp 919,1021,1053, Van Nostrand Reinhold Company Inc., 1985.

5. Haley, Brian K. and Stone, Lawrence D., *Search Theory and Applications*, Proceedings of the NATO Advanced Research Institute on Search Theory and Applications held in Praia Da Rocha, Portugal, March 26-30, 1979, Plenum Press, 1980.

6. Koopmans, Lambert H., *Introduction to Contemporary Statistical Methods*, 2nd ed., pp 352-356, Duxbury Press, 1987.

BIBLIOGRAPHY

Brantley, P., Fox, B. L., and Schrage, L. E., *A Guide to Simulation*, 2nd ed., Springer-Verlag, New York, Inc., 1987.

Chambers, John M., Cleveland, William S., Kleiner, Beat, Tukey, Paul A., *Graphical Methods for Data Analysis*, Wadsworth & Brooks/Cole Advanced Books & Software, 1983.

Conolly, B., and Roberts D, "Random Walk Models for Search with Particular Reference to a Bounded Region", *European Journal of Operational Research*, v. 28, pp 308-320, March 1987.

MODSIM II, The Language for Object-Oriented Programming, Reference Manual, CACI Products Company, 1991.

Operations Evaluation Group, Office of the Chief of Naval Operations, OEG Report No. 56, *Search and Screening*, by Bernard Osgood Koopman, 1946.

Ross, Sheldon M., *Introduction to Probability Models*, 4th ed., Academic Press, Inc., 1989.

Stone, Lawrence D., "Recent Developments and Applications of Optimal Search for Moving Targets," *Operational Research 84*, pp 212-223, 1984.

SIMGRAPHICS II Reference Manual, CACI Products Company, 1991.

INITIAL DISTRIBUTION LIST

1.	Library, Code 52 Naval Postgraduate School Monterey, CA 93943-5002	2
2.	LT William J. Lohr 22 Tall Oaks Rd. East Brunswick, NJ 08816	2
3.	Professor Michael P. Bailey, Code OR/Ba Naval Postgraduate School Monterey, CA 93943-5000	3
4.	Professor James N. Eagle, Code OR/Ea Naval Postgraduate School Monterey, CA 93943-5000	3
6.	Art Turriff STS(STDP) Group John Hopkins University Applied Physics Laboratory Laurel, MD 20707-6099	1
7.	Defense Technical Information Center Cameron Station Alexandria, VA 22304-6145	2
8.	Professor Wayne Hughes, Code OR/Hl Naval Postgraduate School Monterey, CA 93943-5000	1

DUDLEY KNOX LIBRARY
NAVAL POSTGRADUATE SCHOOL
MONTEREY CA 93943-5101

DUDLEY KNOX LIBRARY
3 2768 00309456 6